



THE UNIVERSITY *of* EDINBURGH

Edinburgh Research Explorer

Foot-and-mouth disease virus localisation on follicular dendritic cells and sustained induction of neutralising antibodies is dependent on binding to complement receptors (CR2/CR1)

Citation for published version:

Gordon, L, Mabbott, N, Wells, J, Kulik, L, Juleff, N, Charleston, B & Perez-Martin, E 2022, 'Foot-and-mouth disease virus localisation on follicular dendritic cells and sustained induction of neutralising antibodies is dependent on binding to complement receptors (CR2/CR1)', *PLoS Pathogens*, vol. 1009942, e1009942, pp. 1 - 27. <https://doi.org/10.1371/journal.ppat.1009942>

Digital Object Identifier (DOI):

[10.1371/journal.ppat.1009942](https://doi.org/10.1371/journal.ppat.1009942)

Link:

[Link to publication record in Edinburgh Research Explorer](#)

Document Version:

Peer reviewed version

Published In:

PLoS Pathogens

General rights

Copyright for the publications made accessible via the Edinburgh Research Explorer is retained by the author(s) and / or other copyright owners and it is a condition of accessing these publications that users recognise and abide by the legal requirements associated with these rights.

Take down policy

The University of Edinburgh has made every reasonable effort to ensure that Edinburgh Research Explorer content complies with UK legislation. If you believe that the public display of this file breaches copyright please contact openaccess@ed.ac.uk providing details, and we will remove access to the work immediately and investigate your claim.



1
2
3
4
5
6
7
8
9
10
11
12
13
14
15
16
17
18
19
20
21
22
23

**Foot-and-mouth disease virus localisation on follicular dendritic cells
and sustained induction of neutralising antibodies is dependent on
binding to complement receptors (CR2/CR1)**

Lucy Gordon^{a, b}, Neil Mabbott^b, Joanna Wells^a, Liudmila Kulik^c, Nick Juleff^d, Bryan
Charleston^{a*}, Eva Perez-Martin^a

^aThe Pirbright Institute, Woking, Surrey, United Kingdom

^bThe Roslin Institute and Royal (Dick) School of Veterinary Studies, University of
Edinburgh, Easter Bush, Midlothian, United Kingdom

^cDivision of Rheumatology, Department of Medicine, University of Colorado School of
Medicine, Aurora, Colorado, United States of America

^d Bill and Melinda Gates Foundation, North Seattle, Washington, United States of America

*Corresponding author

E-mail: bryan.charleston@pirbright.ac.uk

24 **Abstract**

25 Previous studies have shown after the resolution of acute infection and viraemia, foot-
26 and-mouth disease virus (FMDV) capsid proteins and/or genome are localised in the light
27 zone of germinal centres of lymphoid tissue in cattle and African buffalo. The pattern of
28 staining for FMDV proteins was consistent with the virus binding to follicular dendritic cells
29 (FDCs). We have now demonstrated a similar pattern of FMDV protein staining in mouse
30 spleens after acute infection and showed FMDV proteins are colocalised with FDCs.
31 Blocking antigen binding to complement receptor type 2 and 1 (CR2/CR1) prior to infection
32 with FMDV significantly reduced the detection of viral proteins on FDCs and FMDV
33 genomic RNA in spleen samples. Blocking the receptors prior to infection also significantly
34 reduced neutralising antibody titres, through significant reduction in their avidity to the
35 FMDV capsid. Therefore, the binding of FMDV to FDCs and sustained induction of
36 neutralising antibody responses are dependent on FMDV binding to CR2/CR1 in mice.

37 **Author Summary**

38 Foot and mouth disease virus causes a highly contagious acute vesicular disease,
39 resulting in more than 50% of cattle, regardless of vaccination status, and almost 100% of
40 African buffalo becoming persistently infected for long periods (months) of time. Yet, the
41 mechanisms associated with establishment of persistent infections are still poorly understood.
42 Post infection, animals are characterised by the presence of long-lived neutralising antibody
43 titres, which contrast with the short-lived response induced by vaccination. We have used a
44 mouse model to understand how foot-and-mouth disease virus is trapped and retained in the
45 spleen for up to 28 days post infection and how the absence of antigen on FDCs correlates
46 with a reduced neutralising antibody response. Our results highlight the potential of targeting
47 antigen to FDCs to stimulate potent neutralising antibody responses after vaccination.

48 **Introduction**

49 One of the features of foot-and-mouth disease virus (FMDV) infection, which has a
50 major impact on the control and eradication of foot-and-mouth disease (FMD), is the
51 existence of the “carrier state” (1, 2). A carrier of FMDV is defined as an animal from which
52 live virus can be recovered from the nasopharynx after 28 days following infection, which
53 frequently occurs in ruminants after acute infection (3). Only ruminants have been shown to
54 become FMDV carriers, and among them, the majority of infected African buffalo become
55 carriers after acute infection and can carry FMDV for up to 5 years or more, which is why
56 African buffalo are considered the primary reservoir of FMDV in Africa (4-7). Over 50% of
57 cattle exposed to FMDV become carriers (4, 5, 8), and although current vaccines prevent
58 clinical disease, they do not prevent primary infection in the nasopharynx, therefore
59 vaccinated animals can still become carriers of FMDV (9).

60 FMDV infection of ruminants elicits the production of specific serum neutralising
61 antibodies which can provide protection for years (6, 10). T cell depletion studies in cattle
62 identified that CD4⁺ T-cell-independent antibody responses are required for resolution of
63 clinical FMD in cattle (11). Similarly, FMDV vaccines induce predominantly CD4⁺ T-
64 independent antibody responses that are enhanced by T cell activation (12). Current
65 inactivated FMD vaccines generally offer only a short-lived immune response in the host, due
66 to the inability to induce FMDV-specific memory B cells. Neither infection nor vaccination
67 induces a significant number of circulating memory B cells, despite a key difference of
68 longer duration of immunity post-infection compared to post-vaccination (13).

69 Antigen retention on stromal follicular dendritic cells (FDCs) has been shown to
70 maintain humoral immune responses by retaining antigen-containing complement-coated

71 immune complexes (ICs) on their surface for long periods of time via complement receptors
72 (CR2/CR1) and/or antibody Fc receptors (14-16). FDCs are specialised immune cells of
73 stromal origin found in the spleen, lymph nodes (LNs) and other lymphoid tissue including
74 tonsil and mucosal surfaces, within B cell follicles in the light zones of germinal centres
75 (GCs) (17). They are necessary for GC formation, lymphoid follicle organisation and
76 promoting B cell proliferation, survival and differentiation (18). FDCs display native
77 antigens within ICs to both naïve and GC B cells; therefore, FDCs are crucial for an effective
78 humoral immune response (19). The longevity of FDCs and their ability to trap and retain
79 antigens in their native forms has also been exploited by certain pathogens. FDCs represent a
80 major extracellular reservoir for a number of viruses and other pathogens including, but not
81 limited to, human immunodeficiency virus (HIV), vesicular stomatitis virus (VSV), bovine
82 viral diarrhoea virus (BVDV) and prions (20-23). Juleff et al. first hypothesised that upon
83 natural infection FMDV binds to and is retained by FDCs in the form of immune-complexed
84 FMDV particles, resulting in prolonged stimulation of the anti-FMDV immune response,
85 which maintain high levels of neutralising antibodies through continual exposure of B cells to
86 FMDV-ICs on FDCs (24). In cattle it was demonstrated that the virus can persist in
87 association with FDCs in the lymphoid tissues of the head and neck (24). These data
88 provided insight into the potential mechanisms of viral persistence and the long-lasting
89 antibody responses seen upon natural infection. An alternative study has described the site of
90 FMDV persistence as pharyngeal epithelial cells in both vaccinated and non-vaccinated
91 persistently infected cattle within the mucosa-associated lymphoid tissue, interestingly
92 associated with CR2⁺ sub-epithelial lymphoid follicles (25). Our previous data have also
93 suggested that in buffalo persistently infected with the Southern African Territories (SAT)
94 FMDV serotypes SAT-1, SAT-2 and SAT-3, quantities of FMDV RNA were significantly
95 higher in the GC-containing regions of lymphoid tissues compared to epithelium samples,

96 which again warranted further investigation into the possibility of virus-persistence in
97 association with FDCs (26).

98 Data from experiments in mice have been fundamental in demonstrating the
99 complement receptor-mediated retention of certain pathogens on FDCs (27, 28). For
100 example, Ho et al. were able to demonstrate the binding of HIV to lymph node FDCs by
101 using a rat monoclonal antibody (mAb) 7G6 to block CR2, which in turn prevented binding
102 and retention of virions (29). This observation was confirmed with the use of CR2/CR1-
103 deficient (*Cr2*^{-/-}) mice, whereby no virus could be detected on FDCs (29).

104 Using a mouse model of FMDV persistence, our previous data suggested that splenic
105 FDCs were able to trap and maintain FMDV for up to 63 days post infection (dpi) (30). The
106 main aim of the current study was to identify the receptor(s) involved in the maintenance of
107 FMDV antigen within the spleen, and whether retention of antigen impacted the generation
108 and maintenance of neutralising antibodies to FMDV in mice. We show that the blocking of
109 CR2/CR1 on FDCs prevented binding and retention of FMDV, strongly suggesting this
110 interaction is mediated by FMDV binding to CR2/CR1. Further investigation using super-
111 resolution microscopy showed significant co-localisation of FMDV antigen with CR2/CR1⁺
112 FDCs in the spleen. Moreover, blocking of CR2/CR1, and consequently absence of FMDV
113 antigen on FDCs, resulted in the significant reduction of neutralising antibody responses to
114 FMDV. A key function of FDCs in the GC reaction is the presentation of antigen, in the
115 form of ICs, to B cells, driving affinity maturation. Blocking CR2/CR1 resulted in antibodies
116 with a reduced capacity to neutralise virus and lower binding affinity to FMD virus-like
117 particles (VLPs) compared to control animals. Until now, CR2/CR1 were not known to bind
118 and maintain FMDV antigen on FDCs, or the impact of antigen retention on the production of
119 high avidity, neutralising antibodies; therefore, knowledge of this interaction could enable a

- 120 targeted approach to vaccine design, through the binding of complement-coated FMDV-ICs
- 121 on FDCs via CR2/CR1 to increase duration of immunity post-vaccination.

122 **Results**

123 **FMDV can only bind *ex vivo* in the form of immune complexes**

124 The binding of FMDV to the FDC network in spleen samples harvested from naïve
125 mice was examined *in situ*. Spleen samples embedded in O.C.T from naïve mice were used
126 to evaluate the ability of FMDV to bind in different forms. The three forms evaluated, all in
127 the presence of complement provided through the addition of normal mouse serum (NMS),
128 were: FMDV antibody (IB11) alone, FMDV antigen (O1/Manisa/TUR/69) alone and FMDV
129 ICs (antibody and antigen). FMDV was only able to bind in clusters typical of FDC
130 networks, as seen in spleen samples following *in vivo* FMDV infections in mice (31), when in
131 the form of ICs. The negative control condition, IB11 FMDV antibody alone with NMS,
132 produced no signal (Figure 1A) and only a small number of isolated cells were positive for
133 FMDV upon addition of antigen alone with NMS (Figure 1B). A bright signal is detected
134 when FMDV antigen, FMDV antibody and NMS have been incubated together for 1 hour, to
135 allow formation of ICs, prior to addition to the spleen samples (Figure 1C).

136

137 **Fig 1. *Ex vivo* FMDV immune complex deposition assays.**

138 Confocal microscopy images of cryosections from naïve mice spleens after addition of
139 different forms of FMDV. (A) FMDV antibody (IB11), (B) FMDV antigen
140 (O1/Manisa/TUR/69) or (C) FMDV ICs (O1/Manisa/TUR/69 antigen and IB11 antibody)
141 were pre-incubated for 1 hour with 5% NMS prior to addition to the cryosections. FMDV
142 (green) was labelled with polyclonal rabbit anti-FMDV-O1 and detected using anti-rabbit
143 488. (A) Absence of signals for FMDV in spleen cryosections when treated with antibody
144 alone, (B) few isolated cells stained positive for FMDV upon addition of antigen alone and

145 (C) large bright green clusters showing the binding of FMDV ICs in the B cell follicles in the
146 spleen. Nuclei stained blue (DAPI). Scale bars = 100µm.

147

148 **Monoclonal antibody (mAb) 4B2 binds CR2/CR1⁺ in Balb/C mice**
149 **and does not affect the proportion of immune cells in the spleen**

150 In order to study antigen retention, a mouse anti-CR2/CR1 mAb 4B2 was used, which
151 had been shown to block CR2/CR1 for up to 6 weeks *in vivo* in C57 Black mice, thus an
152 excellent reagent for studying long term persistence of FMDV on FDCs in mice (32). First,
153 mice were injected with mAb 4B2, or IgG1 as an isotype control, and effects on splenocytes
154 determined by flow cytometry at intervals afterwards up to 35 days post injection. We chose
155 three anti-CR mAbs to test the blocking ability of mAb 4B2 up to 35 days post injection. The
156 most notable reduction was the binding of mAb 7G6 to splenocytes from 2 days post
157 inoculation (Fig 2A). This mAb binds a similar and overlapping epitope on CR1 and CR2 as
158 mAb 4B2 as described previously (32).

159

160 **Fig 2. Flow cytometric analysis of splenocytes from mice treated with mAb 4B2 or**
161 **control IgG, comparing cell subsets and availability of CR.**

162 Flow cytometry was used to identify the availability of complement receptors in mice after
163 treatment with mAb 4B2 and the percentage of cell subsets, compared to control mice treated
164 with IgG1. Spleen samples were taken at (A, D) early time points and (B, E) late time points
165 from mice treated with 4B2 or IgG1 and naïve animals. At the early time points (A) there is a
166 trend whereby mice treated with mAb 4B2 show a smaller number of positive cells to the CR

167 antibodies, compared to the IgG1 or control groups, although this is not significant; 8C12 p =
168 0.312; 7G6 p = 0.061; 7E9 p = 0.194. By the late time points (**B**) mice treated with 4B2 had
169 significantly reduced binding of the three anti-CR antibodies (p = 0.03) to their cells
170 compared to the control mice. A representative histogram (**C**) of the percentage of positive
171 cells for mAb 7G6 at the late time point. The percentage of the different splenic cell subsets
172 CD8 and CD4 T cells, B cells (B220), macrophages (CD169) and dendritic cells (CD11b) (**D**-
173 **E**) remained unchanged after treatment with 4B2 when analysed from both early and late
174 time points after antibody treatment. A representative flow plot (**F**) of the CD8a and CD4
175 positive cells from a mouse from the 4B2 group at a late time point. Naïve animals were used
176 as controls as they were untreated. *p values are 0.03 using the non-parametric Mann-
177 Whitney U test to compare the medians of the two treatment groups.

178

179 Up to 35 days post inoculation mAb 4B2 is still capable of blocking CR, with a
180 significant reduction of anti-CR2/CR1 mAbs binding to splenocytes, as demonstrated not
181 only by mAb 7G6, but mAbs 8C12, which is monospecific to CR1, and 7E9, which binds a
182 different epitope on CR2/CR1 (Fig 2B). This is in alignment with previous data, whereby the
183 blocking effect is not purely due to steric inhibition, but induces a substantial decrease in the
184 expression level of receptors when mAb 4B2 is used *in vivo* (32).

185 Treatment with mAb 4B2 did not affect the abundance of CD8a cytotoxic T cells,
186 CD4 T helper cells, B cells (B220+ cells), marginal zone macrophages (CD169) and
187 monocytes (CD11b), at early or late timepoints (Figs 2D and 2E respectively). Importantly,
188 immunohistochemistry (IHC) analysis showed the presence of CD21/CD35+ FDCs in the
189 spleens of mice treated with mAb 4B2 (Figs 3 and 5). These data are consistent with data
190 from Kulik et al. that also reported that *in vivo* injection of mAb 4B2 does not induce the

191 death of immune cells including FDCs, but leads to substantial blocking of binding of other
192 mAb to CR2 and CR1 (32).

193

194 **Reduced immune complex trapping by FDC in the spleens of mice** 195 **treated with mAb 4B2**

196 We next investigated the effects of *in vivo* mAb 4B2 treatment on the ability of FDCs
197 to trap ICs. Mice were injected with mAb 4B2 (or an IgG1 isotype control) and 1 day later
198 injected with pre-formed peroxidase-anti-peroxidase (PAP) containing ICs which can bind to
199 FDCs *in vivo* via CR2/CR1 (33). Spleen sections were analysed by confocal microscopy 1
200 day later (Fig 3). The presence of CR2/CR1-expressing FDC was detected using mAb 7E9.
201 In control-treated mice, PAP-ICs were consistently detected in association with FDC
202 networks, with 95% of the FDC networks positive for PAP. In contrast, in the spleens of
203 mice treated with mAb 4B2, PAP-ICs were detected in fewer than 2% of the FDC networks
204 examined, similar to the background levels observed in naïve mice (Table 1). This data
205 demonstrates that pre-treatment of mice with mAb 4B2 effectively blocks the retention of ICs
206 by splenic FDCs *in vivo*.

207

208 **Fig 3. Effect of pre-treatment with mAb 4B2 on the binding of PAP on the FDC** 209 **networks in mouse spleen.**

210 BALB/c mice were treated with 500 µg of 4B2 (n=3) or IgG1 (n=4) control 24 hours before
211 immunisation intravenously with peroxidase anti-peroxidase (PAP). Naïve mice were
212 untreated. Spleen samples were collected in O.C.T from mice culled 1-day post inoculation

213 with PAP. **A)** Cryosections were analysed via confocal microscopy for the presence of PAP
214 associated to the FDC network. Confocal microscopy images are arranged in rows and
215 columns according to the treatment and the staining. **B)** Mice from the 4B2 treatment group
216 had significantly less PAP bound to FDCs compared the control group, p value of 0.05 using
217 the non-parametric Mann-Whitney U test to compare the medians of the two treatment
218 groups.

219 **PAP panels:** show PAP labelled green, detected with anti-rabbit 488. PAP was detected in
220 FDC networks in IgG1 control mice, but not in 4B2 treated mice. Absence of signal to PAP
221 in naïve mouse spleen.

222 **FDC Network:** light zone FDCs labelled red with Alexa Fluor 594-conjugated anti-mouse
223 CD21/CD35 (CR2/CR1) antibody, clone 7E9; FDC clusters were detected in all groups.

224 **Macrophages:** marginal zone macrophages surrounding the light zone GC labelled grey with
225 conjugated mAb CD169-APC.

226 **Merged images:** show deposition of PAP within the FDCs network (yellow, co-localisation)
227 of the IgG1 control mice but not in 4B2 treated mice or naïve mice. Nuclei stained blue
228 (DAPI). Scale bars = 50 µm.

229

230 **Table 1. Immunofluorescence examination of FDC networks in mice spleens treated**
231 **with CR block (4B2) or an isotype control (IgG1) 1 day before PAP immunisation.**

Groups	4B2 ^a	IgG1 ^b
Total number of FDC networks imaged	128	166
Number of FDC networks positive for PAP	2	158

Percentage of FDC networks positive for PAP (%)	1.6	95.2
Medians of PAP-positive FDC networks	0.00	95

232 ^an=3 mice

233 ^bn=4 mice

234

235 **CR2/CR1-blockade enhances the viraemia during FMDV**

236 **infection**

237 Next, we determined the effects of mAb 4B2-mediated CR2/CR1-blockade on the
238 viraemia during FMDV infection. Mice were treated with mAb 4B2, or IgG1 as a control,
239 and 1 day later injected with FMDV. By two days after infection a statistically significant,
240 10-fold increase in the viraemia in sera was detected in mAb 4B2-treated mice compared to
241 control-treated mice (Fig 4A). Viral RNA quantification corroborated the plaque assay
242 results, whereby mAb 4B2-treated mice showed a statistically significant, 10-fold increase of
243 viral genome in the serum compared to the control-treated mice (Fig 4B). By 7 dpi the
244 viraemia was cleared in both groups and no detectable virus was detected by plaque assay or
245 qPCR. Naïve mice were used as negative controls and were negative for both the plaque
246 assay and qPCR. These data importantly show that blockade of CR2/CR1 did not affect the
247 ability of the virus to replicate, in fact the CR2/CR1 blockade resulted in a higher titre of
248 virus in sera post-infection with FMDV in mice.

249

250 **Fig 4. Viraemia in 4B2 treated and control-treated mice in response to FMDV infection.**

251 The presence of viraemia in serum samples from mice treated with 4B2 or IgG1 was
252 investigated by (A) plaque assay and (B) qRT-PCR. Serum samples were collected from 4B2

253 and IgG1 treated mice at 2 and 7 dpi. The quantity of virus in the mouse serum at 2 dpi is
254 expressed as (A) log 10 of the number of plaque forming units (PFU) per 1 ml serum and (B)
255 log 10 of the genome copy number (GCN), with CT values ≥ 35 for 3D FMDV deemed
256 negative and recorded as 0. Each data point represents an individual animal, and the line
257 represents the median values. Naïve mice at 2 dpi and all serum samples harvested from 7
258 dpi were negative for viraemia. P values of <0.05 using the non-parametric Mann-Whitney U
259 test to compare the medians of the two treatment groups.

260

261 **CR2/CR1-blockade reduces the trapping and persistence of** 262 **FDMV antigen in the spleen**

263 Next, we determined whether CR2/CR1 blockade similarly impeded the trapping and
264 persistence of FMDV in the spleen. Mice were treated with mAb 4B2 or IgG1, 1 day later
265 injected with FMDV, and spleens (n=8/group) collected at weekly intervals afterwards.
266 Spleens from naïve mice were used as controls. The location of FMDV and FDC networks in
267 the spleens was determined by immunofluorescence confocal microscopy (Fig 5 A-D). We
268 used mAb 7E9 to detect FDC since the treatment of mice with mAb 4B2 does not completely
269 block the binding of mAb 7E9 to CR2/CR1 (Figs 2-3). The total number of FDC networks
270 and whether they were positive or negative for FMDV is represented in Table 2.

271

272 **Fig 5. Effect of pre-treatment with 4B2 preventing the binding of FMDV on FDCs in**
273 **mouse spleens.**

274 Confocal microscopy images are arranged in rows and columns according to the treatment,
275 day post infection and the staining. BALB/c mice treated with 500 µg of either mAb 4B2 or
276 IgG1 control on day -1 before challenge with FMDV. FMDV-infected mouse spleen samples
277 were collected at (A) 7, (B) 14, (C) 21 and (D) 28 dpi from IgG1 control mice and 4B2 mice
278 (n=8 per group per timepoint). Naïve mouse spleens were taken at 7 dpi (n=4) and 28 dpi
279 (n=4).

280 **FMDV panels:** show FMDV protein labelled green with biotinylated llama single domain
281 anti-FMDV 12S antibody VHH-M3 and streptavidin Alexa-Fluor-488. FMDV was detected
282 in the IgG1 control group at all timepoints. FMDV was not detected in the spleens of the
283 4B2 treated group at any of the time points, with the exception of four mice, three harvested
284 at day 14 and one at day 21. There was an absence of signal for FMDV in naïve mouse
285 spleen at all time points.

286 **FDC Network:** show FDCs labelled red with Alexa Fluor 594-conjugated anti-mouse
287 CD21/CD35 (CR2/CR1) antibody, clone 7E9; FDC clusters were detected at all time points
288 in control, 4B2 treated and naïve mice.

289 **Merged images:** show deposition of FMDV within the light zone FDC network of IgG1
290 control mice (yellow – colocalization); but absence of FMDV within the light zone FDC
291 network of 4B2 treated mice and naïve mice (red). Nuclei stained blue (DAPI). Scale bars =
292 50 µm.

293

294 **Table 2. Immunofluorescence examination of mouse spleen treated with mAb 4B2 or**
 295 **control IgG1 for FMDV in FDC networks at 7, 14, 21 and 28 dpi and naïve mice at 7**
 296 **and 28 dpi.**

Groups	4B2 ^a				IgG1 ^a				Naïve ^b	
DPI	7	14	21	28	7	14	21	28	7	28
Number of FDC networks	579	1078	1100	1091	549	1106	1146	1236 ^T	244	575
Number of FDC networks positive for FMDV	10	152	18	3	343	357	258	128	5	10
Percentage FDC networks positive for FMDV (%)	1.73	14.1	1.6	0.3	62.5	32.3	22.5	10.4	2.05	1.7
Medians of FDC networks positive for FMDV	0.83	0.31	0.96	0.00	63.09	32.97	22.64	9.11	1.89	1.76

297 ^an=8 mice per time point

298 ^bn=4 mice per time point

299

300 Despite the differences in FMDV antigen retention on FDCs, the total number of
 301 FDCs from mice in both the IgG1 control group and the mice treated with the CR2/CR1-
 302 blockade were not significantly different (Fig 6A). This confirms data obtained previously
 303 (32), and therefore the significant reduction in FMDV antigen retention in mice pre-treated
 304 with mAb 4B2 is not due to the lack of FDC networks, but specifically as a result of the
 305 blockade of CR2/CR1.

306

307 **Fig 6. Quantification of FMDV antigen and RNA in spleens from 4B2-treated and**
308 **isotype control treated mice detected by confocal microscopy and RT-qPCR.**

309 Spleen samples were collected from BALB/c mice at 7, 14, 21 and 28 dpi
310 (n=8/group/timepoint) following treatment with either mAb 4B2 or IgG1 isotype control one
311 day prior to IP challenge with $10^{6.2}$ TCID₅₀ of FMDV/O/UKG/34/2001. Sections were cut
312 using a cryostat and a cross-section was taken of the spleens by consistently collecting 16
313 sections per animal with an approximate 70µm gap between each section. **A)** FDC networks
314 were visualised, imaged and counted using mAb 7E9, an anti-CR2/CR1 antibody. There
315 were no significant differences in the total number of FDC networks in the group treated with
316 mAb 4B2 compared to the IgG1 isotype control. **B)** FMDV was detected using a biotinylated
317 llama single domain anti-FMDV 12S antibody VHH-M3, and the percentage of FDC
318 networks which were positive for FMDV was calculated. Mice treated with mAb 4B2 had
319 significantly less FMDV in their FDC networks compared to the isotype control mAb, with a
320 P value of ≤ 0.001 from 7, 21 and 28 post infection. **C)** The samples were analysed by RT-
321 qPCR for the presence of FMDV RNA and the results are expressed as copies per 10^8 copies
322 of 18S rRNA. Each data point represents an individual animal, and the line represents the
323 median values. CT values ≥ 35 for 3D FMDV were deemed negative and recorded as 0.
324 Naïve mice (n=4) were tested at 7 and 28 dpi as negative controls. Using the non-parametric
325 Mann-Whitney *U* test to compare the medians of the two groups, at 7 dpi p value of 0.001; 14
326 dpi p value of 0.007; 21 dpi p value of 0.031.

327

328 In IgG1 isotype control treated mice, FMDV antigen was detected in the majority of
329 FDC networks by 7 dpi. Although the number of FMDV-antigen-positive FDC networks

330 gradually declined as the infection progressed, FMDV antigen was detectable in association
331 with approximately 10% of the FDC networks at 28 dpi (Fig 6B). In contrast, no association
332 of FMDV antigen with FDCs above background levels was detected in the spleens of mAb
333 4B2 treated mice, with the exception of 4 mice, suggesting that CR2/CR1-blockade had
334 prevented the trapping and retention of FMDV on FDC.

335

336 Comparison of the presence of viral RNA similarly revealed that CR2/CR1-blockade
337 had prevented the accumulation and persistence of FMDV in the spleen. While high levels of
338 viral RNA were detected in the spleens of control-treated mice until 21 dpi, the levels in 4B2-
339 treated mice were below the detection limit (Fig 6C). However, although FMDV antigen was
340 detectable in association with FDCs in the spleens of control-treated mice by 28 dpi, the
341 levels of viral RNA in whole spleen samples were below the detection limit in all groups at
342 this time. Thus, these data show that trapping and persistence of FMDV antigen is dependent
343 on FMDV binding to FDCs via CR2/CR1.

344

345 **Co-localisation of CR2/CR1 with FMDV**

346 Localisation of FMDV was consistently found in murine spleens within the FDC
347 networks. Further investigation using stimulated emission depletion (STED) microscopy for
348 super-resolution images confirmed that FMDV proteins were predominantly co-localised
349 with CR2/CR1 on FDCs (Fig 7). ImageJ software was used to confirm that the distribution
350 of the CR2/CR1- and FMDV-antigen-associated fluorochromes were preferentially co-
351 localised, compared to that predicted by the null hypothesis that each of these were randomly
352 and independently distributed (33, 34). This analysis confirmed a highly significant and

353 preferential association of the FMDV antigen with CR2/CR1 on FDCs when compared to the
354 null hypothesis that the pixels were randomly distributed (Fig 7B).

355

356 **Fig 7. Co-localisation of FMDV with FDCs.**

357 BALB/c mice were infected with FMDV/O/UKG/34/2001 and high-resolution images were
358 taken of spleen samples using a STED confocal microscope. **A)** Spleen taken from an
359 infected mouse 7 dpi, demonstrating the co-localisation of FMDV (green) with FDCs (red).

360 **B)** Morphometric analysis using ImageJ confirmed that FMDV was preferentially associated
361 with FDCs in spleen tissues (n=7) and significantly greater than the null hypothesis that the
362 pixels were randomly distributed, with a p value of 0.0023.

363

364 **Virus isolation**

365 In order to determine whether the FMDV antigen retained on the FDCs in murine
366 spleens was infectious, an FMDV-susceptible cell line was inoculated with spleen
367 homogenates from FMDV infected animals. The spleens from 7 mice culled at 7 dpi were
368 used: 2 mice pre-treated with the mAb 4B2; 2 mice pre-treated with the IgG1 isotype control
369 and 3 mice which received no prior treatment before infection with FMDV. All samples
370 were negative confirming previous reports, that in the mouse model (31), infectious FMDV
371 could not be detected in whole spleen samples even though antigen could be detected in the
372 FDC networks.

373

374 **CR2/CR1-blockade reduces the generation of neutralising**
375 **antibodies in FMDV infected mice**

376 Since the retention of antigen on FDCs is important for the induction and maintenance
377 of high-titre antibody responses and B cell affinity maturation (14, 35), we next tested the
378 hypothesis that CR2/CR1-blockade in FMDV-infected mice would impede the generation of
379 virus neutralising antibodies. Serum samples were collected from mAb 4B2- or control
380 IgG1-treated FMDV-infected mice and incubated with FMDV-susceptible cells and FMDV
381 for their ability to neutralise the virus.

382 High titres of virus-specific neutralising antibodies were detected in the sera of
383 control IgG1-treated mice by 7 dpi, titres increased by day 14 and these were maintained up
384 to 28 dpi (Fig 8). In contrast, while virus-specific neutralising antibodies were detected in the
385 sera of mAb 4B2-treated mice by 7 dpi, these did not increase at later time points post
386 infection and their titres were significantly reduced when compared to those in the serum of
387 control IgG1-treated mice (Fig 8).

388

389 **Fig 8. Effect of 4B2 treatment on titres of FMDV neutralising antibodies in mouse**
390 **serum.**

391 FMDV neutralising antibodies were evaluated from serum samples taken from BALB/c mice
392 at 7, 14, 21 and 28 dpi with FMDV. Mice had either been pre-treated with mAbs 4B2 or
393 IgG1 1 day prior to FMDV infection. Naïve mice were used as controls. Each data point
394 represents an individual animal, and the line represents the median antibody titre.
395 Neutralising antibody titres are expressed as the serum dilution that neutralised 50% of 100

396 TCID₅₀ of the virus. Using the non-parametric Mann-Whitney *U* test to compare the
397 medians of the two groups, at 14 dpi p value of 0.001, 21 dpi p value of 0.004 and 28 dpi p
398 value of 0.003.

399

400 **CR2/CR1-blockade had no effect on the total IgG/IgM FMDV-** 401 **specific antibody titres**

402 We next used indirect ELISAs to determine the isotypes of the FMDV-specific
403 antibodies produced in the sera of mice from each treatment group. Despite the significant
404 decrease in the level of virus-neutralising antibodies in the sera of the mAb 4B2-treated mice,
405 there were no significant differences in the titre of virus-specific IgG produced at any of the
406 time points analysed (Fig 9A). A FMDV mAb of known concentration was used in the
407 ELISA as a standard to determine the concentration of FMDV-specific IgG in the polyclonal
408 sera (Fig 9B). At 7 dpi, 4 mice from the 4B2 group and 3 mice from the IgG1 group had
409 FMDV-specific IgM antibodies, and as expected no mice had IgM titres after this timepoint
410 (Fig 9C).

411

412 **Fig 9. Effect of 4B2 treatment on titres of FMDV specific antibodies.**

413 FMDV-specific antibodies in serum samples from mice treated with mAb 4B2 or an isotype
414 control antibody (IgG1) were detected by ELISA. Serum samples were collected at 7, 14, 21
415 and 28 dpi and tested for (A, B) IgG and (C) IgM antibodies. Naïve sera were included on all
416 ELISA plates and the cut-off was set at 1.5 times the OD of the naïve sera. Antibody titres
417 were either expressed as (A, C) the reciprocal log₁₀ of the last positive dilution or (B) using a

418 known FMDV IgG standard to plot the concentration of IgG antibodies in mg/ml. Each data
419 point represents an individual animal, and the bars represent median values. Using the non-
420 parametric Mann-Whitney *U* test to compare the medians of the two groups, there were no
421 statistically significant differences at any time points.

422

423 **CR2/CR1-blockade reduces antibody titres to the neutralising** 424 **FMDV G-H loop**

425 Next, an ELISA was carried out to compare the antibody titres in the mAb 4B2-
426 treatment group and the control group against the O/UKG/12/2001 VP1₁₂₉₋₁₆₉ G-H loop (Fig
427 10A). In mice, the G-H loop is a neutralising epitope of FMDV, and a G-H loop peptide
428 vaccine is sufficient to protect against FMDV challenge (36, 37). Mice treated with mAb
429 4B2 had significantly lower antibody titres to the G-H loop compared to the control group,
430 which may have contributed to the decreased ability of the antibodies from the 4B2-treated
431 mice to neutralise FMDV. However, addition of G-H loop peptide to inhibit the G-H loop
432 activity in mouse sera did not significantly reduce the titre of the VNT assays; therefore, virus
433 neutralisation is not solely conferred by binding to the GH-loop.

434

435 **Fig 10. Effect of 4B2 treatment on titres of IgG antibodies specific to the FMDV G-H** 436 **loop and the avidity of FMDV specific IgG antibodies in mouse serum.**

437 BALB/c mice treated with 500 µg of either mAb 4B2 or IgG1 control on day -1 before
438 challenge with FMDV and sera was collected at 7, 14, 21 and 28 dpi. A) An indirect peptide
439 ELISA showed that mice treated with 4B2 had significantly less antibodies to the FMDV G-

440 H loop compared to the IgG1 control group, with a P value of ≤ 0.05 using the non-parametric
441 Mann-Whitney *U* test. Naïve sera were included on all ELISA plates and the cut-off was set
442 at 1.5 times the OD of the naïve sera. **B)** The avidity of antibodies was measured using
443 biolayer interferometry and was performed using an Octet Red96e. FMD
444 O1/Manisa/TUR/69 VLP were bound to streptavidin sensors and dipped into three dilutions
445 of sera per mouse. Each data point represents the mean avidity of these measurements for
446 each individual mouse, represented as $-\text{Log}_{10}$ of the K_D (M) value. Sera which produced a
447 negative response rate, and therefore had too few antibodies bound to FMD VLPs to reach
448 the limit of detection, are recorded as 0. The results demonstrate that mice treated with 4B2
449 had significantly lower avidity antibodies compared to the control group, with a P value of
450 ≤ 0.05 using the non-parametric Mann-Whitney *U* test.

451

452 **CR2/CR1-blockade decreases antibody avidity to FMD VLPs**

453 We then investigated whether CR2/CR1-blockade had affected the avidity of the
454 FMDV-specific antibodies for FMDV antigen (Fig 10B). Using the data shown in Fig 9B,
455 known concentrations of FMDV-specific IgG in polyclonal sera from infected mice from
456 each group were incubated with stable FMD VLP and the antibody dissociation/association
457 rates ($k_{\text{off}}/k_{\text{on}}$) rates and K_D values determined. The K_D is the equilibrium dissociation
458 constant between an antibody and its antigen and is measured using the ratio of $k_{\text{off}}/k_{\text{on}}$,
459 therefore K_D values were used to represent the avidity of the polyclonal antibodies, based on
460 the individual affinities of the antibodies in the polyclonal serum samples, to the FMD
461 VLP. These data clearly showed that the K_D values in the sera of mice treated with mAb 4B2
462 were significantly lower than those in the sera of IgG1-treated control mice (Fig 10B);
463 suggesting that virus-specific antibodies induced after CR2/CR1-blockade had reduced

464 avidity to FMD VLP. This decrease in antibody avidity to the FMD capsid is likely the
465 predominant cause of the reduced capacity of the antibodies generated after the CR2/CR1
466 blockade to neutralise FMDV, when compared to the control animals (Fig 8).

467 **Discussion**

468 Our previous studies suggested that in cattle FMDV is localised on FDCs in the B cell
469 follicles (24). Similar to studies with HIV where the interaction of virus with FDCs has been
470 explored in detail in mice, we have demonstrated FMDV localises to FDCs in mice after the
471 resolution of viraemia. The mouse model for FMDV persistence showed FMDV antigen
472 retention in the spleen in association with FDC for up to 63 dpi (31). We have now used this
473 FMDV mouse model to gain novel insight into the mechanisms of FMDV persistence on
474 FDCs. In this study, FMDV protein was detected in FDC networks up to 28 dpi and FMDV
475 genome up to 21 days in spleen samples. We suspect the absence of detectable genome at 28
476 days is because the RNA will be in a small number of localised deposits in association with
477 the FDC which may not be detected when the whole spleen is sampled. We have shown
478 previously in cattle and African buffalo that FMDV genome does persist in the GC-
479 containing regions of infected lymphoid tissues for prolonged periods (24, 26).

480 The absence of FMDV antigen and genome by IHC and PCR in mice treated with
481 mAb 4B2 as reported here, demonstrates the role of CR2/CR1 as the major receptor involved
482 in the trapping and retention of FMDV. Our data demonstrating no loss in viraemia is an
483 important observation to show that the mAb 4B2 does not prevent viral replication, and
484 therefore is not the reason for the lack of FMDV detection on the FDC networks in the
485 animals treated with the CR2/CR1 blockade. In fact, our results showed that this blockade
486 increased viraemia in these mice, and although we are not certain why, one hypothesis is that
487 virus was unable to be cleared from the blood as effectively when CR2/CR1 was blocked.

488 Furthermore, blocking of CR2/CR1 results in a significant reduction of neutralising
489 antibody titres against FMDV. Although two mechanisms have been described for antigen

490 trapping by FDC, CR mediated (15) and FcR mediated (38), the near complete elimination of
491 FMDV on FDCs after treatment with mAb 4B2 leads us to believe the trapping is
492 predominantly CR2/CR1-dependent. However, we do not exclude that longer persistence of
493 the virus on FDCs after natural infections, when anti-virus antibody forms, are due to a
494 combination of FcR and CR2/CR1 binding.

495 Ochsenein et al. used *Cr2*^{-/-} mice to investigate antibody responses to a T-
496 independent antigen, VSV. They showed similar findings, that early antibody responses to
497 infection were unaffected in these knockout mice, including no significant effect on the IgM
498 response to infection in mice deficient in CR2/CR1. However, longer term antibody
499 responses to VSV were not significantly different in *Cr2*^{-/-} mice compared to the wild type
500 (WT) (39). Unlike FMDV (13), VSV is able to induce B cell memory, therefore, the contrast
501 to our findings could be because the induction of antibody responses to VSV are less
502 dependent on antigen persistence on FDCs compared to FMDV. The murine *Cr2* gene
503 encodes two proteins, CR1 and CR2, via alternative splicing (40), therefore inactivation of
504 the *Cr2* gene leads to deficiency in both CR1 and CR2. The similarity in these receptors also
505 leads to blocking of both CR1 and CR2 upon administration of an anti-CR2 and/or -CR1
506 mAb.

507 *Cr2*^{-/-} mice have abnormalities in the maturation of GCs including the GC B cells
508 associated with the CR2/CR1 deficiency, which may complicate the interpretation of some
509 studies where they are used. These *Cr2*^{-/-} mice have been shown in multiple studies to have a
510 discernible impairment in their ability to mount a humoral immune response (41, 42). A
511 recent study by Anania et al. used image analysis to demonstrate that FDCs lacking CR1 and
512 CR2 not only have a decreased ability to capture ICs, but in the *Cr2*^{-/-} mice, GCs are fewer
513 and smaller and FDCs are poorly organised (43). FDCs use chemokine gradients within the

514 B cell follicles to interact with B cells and T follicular helper, therefore disorganisation of the
515 FDC networks leads to a variety of abnormalities, including impaired B cell survival and
516 reduced Ig production (44).

517 Although *Cr2*^{-/-} mice are unable to mount a normal humoral immune response to
518 various antigens, a study showed that *Cr2*^{-/-} mice had reportedly normal levels of total IgM
519 and of the different IgG isotypes, showing no evidence of altered B- or T- cell development
520 (42). These studies showed antibody titres were similar in *Cr2*^{-/-} and wildtype (WT) mice,
521 however functional differences in antibodies were not specifically investigated. We also
522 showed IgM and IgG titres were similar in treated and control mice, but went on to show low
523 avidity, non-neutralising antibodies were produced which could be due to a defective affinity
524 maturation process due to the lack of binding of FMDV proteins to CR2/CR1 on FDCs.
525 Furthermore, it has been established that in mice the G-H loop is a neutralising epitope
526 inducing protection against FMDV (36); and mice treated with mAb 4B2 had a modest
527 reduction of antibodies to the G-H loop. These results correlate with the reduced ability of
528 the antibodies from the mice treated with 4B2 to neutralise FMDV from 7 dpi, although the
529 reduction in avidity of the FMDV-specific antibodies appears to be the predominant reason
530 for the differences in the virus neutralisation between the 2 groups.

531 Due to the off-target effects from using *Cr2*^{-/-} knockout mice to study the function of
532 FMDV antigen on FDC, we used the mAb 4B2 to block CR2/CR1 on FDCs. This antibody
533 had been previously described to block these receptors for up to 6 weeks *in vivo* in mice,
534 without disrupting other cell types. Bioimaging and flow cytometry analysis confirmed that
535 the number and size of FDC networks were normal, and the percentage of other immune cell
536 subsets in the spleen, including B- and T- cells were unaltered after blocking up to 35 days.

537 We were therefore confident that the mAb 4B2 treatment would indicate whether antigen
538 bound to CR2/CR1 on FDCs impacted on the immune response.

539 A number of studies have used *Cr2*^{-/-} mice and reconstituted with *Cr2*^{+/+} WT bone
540 marrow (BM) to allow a more specific investigation of the role of CR2/CR1 on FDCs
541 without impairing B cell functions (45-47). This is possible because FDCs are derived from
542 stromal cells, whereas B cells are BM in origin. Initial IgG and IgM responses were shown
543 to be similar in *Cr2*^{-/-} mice with or without WT BM (*Cr2*^{+/+} B cells), suggesting antigen can
544 induce a B cell response in the absence of CR expression (45, 46). However, studies
545 investigating the long-term antibody response of these chimeric mice have shown a
546 significant reduction in both long-term antibody production and memory when FDCs
547 specifically did not express *Cr2* (46, 47). This is in line with our results where neutralising
548 antibody responses up to day 7 post infection were similar in mice with or without a
549 CR2/CR1 block, yet after this timepoint, there was a significant reduction in FMDV
550 neutralising antibodies in mice treated with the anti-CR2/CR1 mAb.

551 It is well established that CR1 and CR2 are essential for binding ICs and are
552 expressed at high levels on FDCs; and while FDCs can also trap ICs via the FcR, it is to a
553 lesser degree [14-16, 48]. FDCs can acquire antigen through various pathways, including
554 direct interaction by small antigens as well as by binding to complement component 3 (C3)
555 fragments on ICs via CR2/CR1 when presented to them via B cells (17, 48). It has been
556 previously described that C3 fragments, specifically C3d, could therefore be used as a
557 vaccine adjuvant (49). A study by Ross et al. demonstrated the effectiveness of C3d-fusions
558 to Influenza virus haemagglutinin in enhancing antibody production and maturation, leading
559 to a protective immune response in the influenza mouse model (50). This would be a
560 particularly interesting area of research for FMDV, due to the short duration of immunity

561 after FMD vaccination. If fusion of C3d to FMD vaccine antigens resulted in targeted
562 antigen deposition on FDCs, this could improve the magnitude and duration of the
563 neutralising antibody response.

564 Similar to other studies with FMDV (31), we have been unable to demonstrate that
565 FMDV retained by FDCs in mice is infectious. Furthermore, in cattle persistently infected
566 with FMDV, viral non-structural proteins associated with viral replication were not detected
567 in the GC-containing regions of lymphoid tissues, therefore suggesting that persisting FMDV
568 antigen, likely associated to FDCs, is non-replicative (24). Bachmann et al. reported similar
569 findings with VSV, that whilst VSV was not infectious on FDCs, the long duration of
570 immunity seen was possible due to FDCs trapping and retaining antigen for long periods of
571 time (20). Therefore, despite the presence of FMDV on FDCs for long periods of time, this is
572 in a non-infectious form, thus indicating a potential for non-infectious vaccines to reproduce
573 this persistence to enhance the duration of immunity by eliciting FMDV-specific antibodies
574 without the need for infectious virus.

575 Although the current study has highlighted the role of FDCs in the maintenance of
576 neutralising antibodies to FMDV, further experiments are required to delineate GC and
577 extrafollicular responses in order to understand how FMDV persistence results in the
578 generation and maintenance of the specific immune response in greater detail. Studies have
579 shown that low-affinity plasmablasts are produced in transient primary extrafollicular foci,
580 prior to somatic hypermutation and affinity maturation in GCs (51-54). Therefore, up to 7
581 dpi the lack of significant differences in the results between 4B2 treated and control mice
582 could be because of an extracellular, GC-independent response in both groups, which would
583 also explain the low avidity of antibodies to the FMD capsid as shown by BLI. Although Ig
584 class switching occurs extrafollicularly, there is evidence of only low-level hypermutation,

585 thus the production of low affinity B cells in the initial stages of infection (55-57).
586 Consequently, the mAb 4B2 may have a lesser effect in the early stages of the adaptive
587 immune response, where the GC reaction and FDCs are less involved. Furthermore, the
588 similar titres of antibodies seen in both groups from 14 dpi could indicate a long-term
589 extrafollicular response in the mAb 4B2 treated group, where plasma cells are produced, but
590 the affinity maturation process is less effective than in the GC, which is then reflected in the
591 lower avidity antibodies produced in mice treated with mAb 4B2 compared to the control
592 mice. A review by Elsner et al. highlighted potential factors which could be studied to help
593 understand the FMDV GC and extrafollicular responses in more detail (58). For example,
594 interleukin (IL)-12 has been shown to block T follicular helper cells (Tfh) and suppress GCs,
595 resulting in an extrafollicular dominant response. Whereas, IL-6 promotes early GC
596 reactions by promoting Tfh and blocking Th1.

597 Our study provides new insight into the immune pathogenesis of FMDV by
598 demonstrating the interaction of the virus with FDCs. Studies in cattle and African buffalo
599 have shown the virus localises to GC-containing regions of lymphoid tissues after the
600 resolution of acute infection, but now we have demonstrated that FMDV binds as an IC to
601 FDCs via CR2/CR1 in mice. We have also shown this interaction is crucial for the production
602 of high avidity neutralising antibodies after FMDV infection. Furthermore, when CR2/CR1
603 is blocked, there is a significant reduction in the avidity of antibodies and a significant
604 reduction in FMDV neutralising responses in serum. Short duration of immunity is one of the
605 major problems with current killed FMDV vaccines, these studies provide insights into how
606 the duration of protective antibody responses may be increased post-vaccination.

607 **Materials and Methods**

608 **Mice and experiment design**

609 Experiments were carried out to address 3 objectives; firstly, to determine whether the mAb
610 4B2 successfully blocked CR2/CR1 by using PAP which is known to bind to FDCs via the
611 CR2/CR1. Secondly, to determine the effect of 4B2 on the cell subsets of the spleen.
612 Finally, a challenge study to determine whether FMDV needs to bind to FDCs via the
613 CR2/CR1 to maintain a neutralising antibody response. Female BALB/c mice (8-12 weeks)
614 were used in these experiments and were purchased from Charles River Laboratories, UK.
615 Mice were acclimatised for 7 days before being used in experiments and were maintained
616 with food and water ad-libitum and full environmental enrichment. Mice were humanely
617 culled using isoflurane and a rising concentration of carbon dioxide (CO₂) method. All
618 animal experiments were performed in the animal isolation facilities at the Pirbright institute
619 and were conducted in compliance with the Home Office Animals (scientific procedures)
620 ACT 1986 and approved by the Pirbright Institute's Animal Welfare and Ethical Review
621 Board (AWERB). Naïve mice were used as negative controls throughout the study and
622 remained untreated and were not infected with FMDV.

623 **4B2 treatment:** BALB/c mice were given a single intraperitoneal (i.p.) injection of
624 200µl of 0.5 mg purified mAb 4B2 to mouse CR2/CR1 (32). Animals treated with the same
625 dose of a mAb anti-OVA IgG1, F2.3.58 antibody (2B Scientific, UK) were used as isotype
626 matched controls. Two mice treated with 4B2 and two with the IgG1 control mAb were
627 culled at 2- and 7-days post treatment “early time points”, and a further two from each group
628 at 22- and 35-days post treatment “late time points” to assess the effects of 4B2 on spleen cell

629 subsets. The spleen samples were collected in RPMI media (Gibco, UK) and immediately
630 processed in the lab for flow cytometry.

631 **PAP treatment:** To test the ability of 4B2 to block CR2/CR1 *in vivo*, mice were given
632 a single injection of 100µl preformed rabbit peroxidase-anti-peroxidase (PAP) immune
633 complexes (Sigma) intravenously 1 day after treatment with 4B2 (n=4) or anti-OVA IgG1
634 (n=4). Mice were culled 1 day later, and their spleens were collected in optimal cutting
635 temperature (OCT) compound (VWR Chemicals, UK) and stored at -80° C to test for the
636 presence of FDC-associated IC by confocal microscopy.

637 **FMDV infection:** 1 day after treatment with mAbs 4B2 or IgG1, mice were inoculated
638 i.p. with a total dose of $10^{6.2}$ TCID₅₀ of FMDV/O/UKG/34/2001 in 200µl. After challenge,
639 mice were bled from the tail vein at 2, 7, 14, 21 and 28 dpi. Terminal bleeding after culling
640 from cardiac puncture and spleens from culled mice were collected from 8 animals at 7, 14,
641 21 and 28 dpi from each treatment group. The spleens were cut in half, with half collected in
642 OCT for analysis by confocal microscopy and half collected in RPMI medium (Gibco, UK)
643 for analysis by PCR. The whole blood samples were stored at 4° C overnight to allow blood
644 clotting, the samples were centrifuged, and the serum was collected and stored at -80° C.

645 **FMDV immune complex deposition**

646 Spleens from naïve BALB/c mice embedded in OCT were cut using a cryostat (7-9
647 µm) and sections mounted on a superfrost slides. The samples were blocked with 5% normal
648 goat serum (NGS) (abcam, UK) for 30 minutes prior to addition of ICs and controls. The
649 FMDV ICs consisted of inactivated O1/Manisa/TUR/69 FMDV vaccine antigen and IBII
650 FMDV O antibody at 1:1 ratio and incubated with NMS, providing the necessary
651 complement, for 30 minutes. The controls were O1/Manisa/TUR/69 antigen or IBII FMDV

652 O antibody with only the addition of complement in the form of NMS. The ICs and controls
653 were diluted in PBS 1:10, resulting in a final concentration of 5% NMS, and added to the
654 tissue sections for 1 hour at room temperature. The slides were washed and fixed with fixed
655 with 4% paraformaldehyde for 20 minutes. A polyclonal rabbit anti-O FMDV was added to
656 the slides for 1 hour at room temperature to detect FMDV ICs bound to the cryosections. The
657 slides were washed and 4 µg/ml goat anti-rabbit IgG (H+L) cross-adsorbed secondary
658 antibody, Alexa Fluor 488 (Invitrogen) was added for 1 hour at room temperature in the dark.
659 The sections were counterstained with DAPI to distinguish cell nuclei. Spleen sections were
660 visualised, imaged and all data was collected using a Leica SP8 confocal microscope (Leica
661 Microsystems GmbH, Germany).

662 **Processing splenocytes**

663 The spleen samples collected in RPMI medium were homogenised and passed
664 through 70 µm cell mesh strainers (BD Biosciences, UK). Cells were washed in RPMI
665 medium by centrifugation and red blood cells were lysed with ACK lysing buffer (Sigma-
666 Aldrich, UK). Following lysis, cells were washed twice in RPMI by centrifugation and re-
667 suspended in RPMI complete medium (RPMI with 10% foetal bovine serum (Gibco, UK),
668 1% Gibco penicillin-streptomycin (10,000 U/ml) (Life Technologies, UK) and 1% Gibco
669 MEM non-essential amino acids (100X) (Life Technologies, UK)), counted and stored at 4°
670 C overnight prior to flow cytometric analysis.

671 **Flow Cytometry**

672 The processed splenocytes were distributed at 1×10^6 per well into Nunc 96-well
673 round bottom microwell plates (Thermo Scientific, UK). The cells were blocked by adding
674 5µg/ml purified rat anti-mouse CD16/CD32 (mouse BD Fc Block) clone: 2.4G2 (BD

675 Biosciences, UK) in autoMACS buffer (Miltenyi Biotec, UK). Cells were stained with
676 CD8a-FITC (Life Technologies), CD4-PE (Miltenyi Biotec) to detect cytotoxic and helper T
677 cells respectively and B220 biotin RA3-6B2 Alexa Fluor 647 to detect B cells (CD45R),
678 CD11b-APC to detect dendritic cells and CD169 (Siglec-1)-APC to detect marginal zone
679 macrophages. Streptavidin Molecular Probe Alexa-Fluor-633 conjugated secondary mAb
680 (1µg/ml) (Invitrogen) was used to detect biotinylated antibodies 7E9 (BioLegend, UK) and
681 7G6 (BD Biosciences, UK) to identify CD21/CD35 (CR2/CR1) and 8C12 (BD Biosciences,
682 UK) to identify CD35 (CR1). Single staining controls and no staining controls were also
683 included for compensation purposes. The cells were then fixed with 1% paraformaldehyde,
684 washed and resuspended in MACS buffer, before being read on the MACS Quant (Miltenyi
685 Biotec, UK). The analysis was completed using FCS Express (De Novo Software, US).

686 **Quantification of viraemia by plaque assay**

687 Foetal goat tongue cells (ZZR cells), which are highly susceptible to FMDV, were
688 grown up to 95-100% confluency in 6 well plates. Cells were washed in PBS and a 10-fold
689 dilution of serum samples from 2 dpi (n=30 and n=22 from 4B2 and IgG1 treatment group,
690 respectively) and 7 dpi (n=4 per treatment group) were added to the wells. Serum from 2
691 naïve animals at 2 dpi and 1 naïve animal at 7 dpi were used as negative controls. Plates
692 were incubated for 30 minutes at 37°C with 5% CO₂ and then 3ml/well of Eagle's Overlay-
693 Agarose (Eagle's overlay media (TPI, UK) and 2% agarose (Sigma, UK)) was added and
694 allowed to set at room temperature. Plates were incubated at 37°C with 5% CO₂ for 48 hours.
695 Following incubation, plates were fixed, and plaques visualized by staining the cell
696 monolayer with methylene blue in 4% formaldehyde in PBS for 24 hours at room
697 temperature. The plates were washed with water and the agarose plugs discarded. The
698 viraemia was expressed as the Log₁₀ of the number of plaque forming units per ml (PFU/ml).

699 **One Step RT-qPCR of serum samples**

700 Due to low volumes of serum collected from the tail vein, serum samples from
701 animals taken at 2 dpi were pooled to reach 50µl. Therefore, FMDV genome copy number
702 was measured by RT-qPCR in 6 pools of serum from IgG1 and 4B2 treated mice and 3 pools
703 from the naïve groups. Fifty µl of serum samples taken from terminal bleeds from culled
704 animals at 7 dpi were also analysed. The RNA was extracted using the MagVet Universal
705 Isolation Kit (Thermo Fisher Scientific, UK) and the KingFisher Flex (Thermo Fisher
706 Scientific, UK). The PCR was performed, using the SuperScript III Platinum One-Step
707 Callahan 3D quantitative RT- qPCR, according to the standard protocol of the World
708 Referenced Laboratory for FMDV, with a cut-off cycle threshold (Ct) of ≥ 35 (59). Results
709 were expressed as Log₁₀ FMDV genome copy number (GCN)/ml of sample by extrapolating
710 the Ct values to GCN by using a linear regression model with serial dilutions of in vitro
711 synthesized 3D RNA standard.

712 **RT-qPCR from tissues**

713 Spleen samples were homogenised in 200µl DMEM media (Gibco, UK) using the
714 FastPrep-24 and lysing matrix tubes (MP Biomedicals) prior to RNA extraction (as described
715 above). Following RNA extraction, cDNA was generated using TaqMan reverse
716 transcription reagents (Applied Biosystems, UK,). The EXPRESS qPCR SuperMix
717 Universal Kit (Invitrogen, UK) was used for real time-PCR and the PCR reactions for FMDV
718 3D were performed as previously described, with a cut-off cycle threshold (CT) of ≥ 35 (59).
719 The 18S ribosomal RNA housekeeping gene was used for normalisation based on previously
720 published primers (60, 61). The PCR reaction was performed on a Stratagene MX3005p

721 quantitative PCR instrument (Stratagene, USA). Results were expressed as Log₁₀ FMDV
722 RNA copies/10⁸ copies 18S.

723 **Immunofluorescence by confocal microscopy**

724 The frozen spleens embedded in OCT were cut on a cryostat (7-9 µm), mounted on a
725 superfrost slide and stored at -20° C overnight. The slides were air-dried, fixed with 4%
726 paraformaldehyde and blocked with 5% NGS (abcam, UK). FDC networks visualised by
727 staining with 1µg/ml Alexa Fluor 594-conjugated anti-mouse CD21/CD35 (CR2/CR1)
728 antibody, clone 7E9 (BioLegend, UK), marginal zone macrophages were visualised using
729 1µg/ml CD169 (Siglec-1), clone MOMA-1 (Bio-Rad, UK), 2µg/ml biotinylated llama single
730 domain anti-FMDV 12S antibody VHH-M3 (Kindly provided by Dr M Harmsen, Central
731 Veterinary Institute of Wageningen, AB Lelystad, The Netherlands) (62) was used to detect
732 FMDV/O/UKG/34/2001 and goat anti-rabbit Molecular Probe Alexa-Fluor-488 was used to
733 detect PAP IC. Goat anti-rat and streptavidin Molecular Probes Alexa-Fluor-488 and 633
734 conjugated secondary mAbs (Invitrogen) were used at 2µg/ml and all sections were
735 counterstained with DAPI to distinguish cell nuclei. Spleen sections were visualised, imaged
736 and all data was collected using a Leica SP8 confocal microscope (Leica Microsystems
737 GmbH, Germany).

738 The same protocol was used for the stimulated emission depletion (STED) with the
739 following changes: goat anti-rat and streptavidin Molecular Probes Alexa-Fluor-488 and 555
740 conjugated secondary mAbs (Invitrogen) were used at 4µg/ml, ToPro3 was used for nuclear
741 staining and a super-resolution Leica TCS SP8 STED 3X microscope (Leica Microsystems
742 GmbH, Germany) equipped with 592 and 660nm depletion lasers was used to image and
743 collect data. STED images were then deconvolved in Huygens Professional software 21.04
744 (Scientific Volume Imaging, Netherlands) using the Deconvolution Wizard with a theoretical

745 PSF. Data was analysed using ImageJ software as previously described (33, 34) to compare
746 the null hypothesis (that the pixels were randomly distributed) to the observed levels of co-
747 localisation.

748 **Virus Isolation**

749 Virus isolation was carried out to determine whether FMDV persisting in the murine
750 spleens was infectious. Spleens were homogenised using FastPrep Lysing Matrix D tubes
751 with the FastPrep-24 (MP Biomedicals). The spleen homogenate was then added to T25
752 flasks containing ZZR cells (goat tongue epithelial cells), which are susceptible to FMDV.
753 The cells and homogenate were incubated at 37°C in 5% CO₂ and checked daily for
754 cytopathic effect (CPE). After 48 hours the flasks were stored at -20°C, and once frozen were
755 defrosted, centrifuged and supernatant was collected. The supernatant from each sample was
756 then added to new flasks of confluent ZZR cells and the process was repeated for a total of 3
757 passages. The presence of CPEs would demonstrate that the FMDV was infectious, absence
758 of CPEs would demonstrate no infectious FMDV. A flask inoculated with FMDV-OUKG
759 and a flask of ZZR cells only were used as positive and negative controls respectively for
760 each passage.

761 **Virus Neutralising Test**

762 Serum samples collected at 7, 14, 21 and 28 dpi were heated at 56° C for 1 hour to
763 inactivate complement and analysed for their ability to neutralise a fixed dose of FMDV on
764 IB-RS-2 cells (porcine cells). Samples were then diluted 2-fold in 96 well plates in duplicate
765 in serum free medium starting from a 1:8 dilution. Naïve mouse serum and cells only were
766 used as negative controls. One hundred tissue culture infectious dose 50 (TCID₅₀) of FMDV
767 OUKG was added to all wells excluding cell only controls. Plates were incubated for 1 hour

768 at room temperature before 5×10^4 IB-RS-2 cells were dispensed to each well. The plates
769 were incubated at 37°C in 5% CO₂ and checked daily for cytopathic effect (CPE). After 72
770 hours the plates were inactivated with 1% Trichloroacetic acid (TCA) (Sigma-Aldrich, UK)
771 washed with water and stained with methylene blue. Neutralising antibody titre was
772 calculated using the Spearman-Kärber formula and results expressed as the log₁₀ reciprocal
773 serum dilution that neutralised 50% of 100 TCID₅₀ of the virus (63).

774 **IgG and IgM ELISA**

775 An indirect enzyme-linked immunosorbent assay (ELISA) was developed to detect
776 FMDV-specific mouse antibodies. The assay was adapted from the FMDV isotype specific
777 ELISA protocol to detect antibodies to FMDV in cattle and swine serum (11). ELISA plates
778 were coated with a rabbit anti-O FMDV polyclonal antibody (TPI, UK), washed with PBS
779 containing 0.05% Tween20 (Sigma, UK) and then 0.5 µg/ml inactivated FMDV
780 O1/Manisa/TUR/69 vaccine antigen (Merial, UK), diluted in blocking buffer (1:1 PBS and
781 SEA BLOCK (Thermo Scientific, UK)), was added to each well. Serum samples were
782 added, and bound antibodies were detected by incubating the plates with horseradish
783 peroxidase-conjugated goat anti-mouse IgG or IgM (Invitrogen, UK), diluted in blocking
784 buffer. TMB substrate (Thermo Scientific, UK) was used as a developer and the reaction was
785 stopped with 0.3M H₂SO₄ and the optical density (OD) was read at 450 nm. Antibody titres
786 were expressed as either log₁₀ of the reciprocal of the last dilution with a mean OD greater
787 than 1.5 times the mean of the OD of the negative control serum or using an FMDV-specific
788 IgG standard (IB11 mAb (11)) of known concentration, a standard curve was generated to
789 determine the concentration of the FMDV-specific IgG in the serum samples analysed. The
790 O1/Manisa/TUR/69 vaccine antigen was used due to good cross-reactivity and cross-
791 protection with OUKG as demonstrated in previous studies (64-66).

792 **Peptide ELISA**

793 An indirect peptide ELISA using a biotinylated O/UKG/12/2001 G-H loop peptide
794 (VYNGNCKYGESPVTNVRGDLQVLAQKAARTLPTSFNYGAIK) (Peptide Protein Research
795 Ltd, UK) was developed to determine the presence of antibodies directed against the FMDV
796 VP1₁₂₉₋₁₆₉ G-H loop. The highest concentration of each serum sample was also tested with a
797 biotinylated negative control peptide with a similar molecular weight and number of charged
798 residues vs hydrophobic residues (PSRDYSHYYTTIQDLRDKILGATIENSRIVLQIDNARLA)
799 (Peptide Protein Research Ltd, UK) to ensure the sera wasn't binding non-specifically.
800 Streptavidin coated ELISA plates (Thermo Scientific) were incubated with 8 µg/ml G-H loop
801 peptide diluted in PBS at 37°C for 2 hours. The plates were washed with TBS containing
802 0.1% BSA 0.05% Tween20 (Sigma, UK) and then serum samples were added in duplicate.
803 Bound antibodies were detected by horseradish peroxidase-conjugated goat anti-mouse IgG
804 (Invitrogen, UK) and SIGMAFAST OPD (o-Phenylenediamine dihydrochloride) (Sigma,
805 UK). The optical densities (OD) were measured at 450nm, and antibody titres were
806 expressed as log₁₀ of the reciprocal of the last dilution with a mean OD greater than 1.5
807 times the mean of the OD of the negative control serum.

808 **Biolayer Interferometry**

809 Biolayer interferometry was performed using an Octet Red96e instrument (ForteBio,
810 Inc.) and ForteBio Data Analysis HT software (v 11.1.0.25) was used to determine the
811 response rate, k_{off}/k_{on} rates and the K_D (M) values. This method was adapted from previously
812 described methods using polyclonal sera (67, 68). A 5 µg/ml concentration of biotinylated
813 stable O1/Manisa/TUR/69 FMD VLP (69) (kindly provided by Alison Burman) was
814 immobilised on streptavidin-coated biosensors (Sartorius UK Limited) for 900 s. A baseline

815 was established by measurements taken when sensors were immersed for 60 s in HEPES 10
816 mM, NaCl 150 mM, EDTA 3 mM, 0.005% Tween 20 (HBS-EP) buffer (Teknova). The
817 sensors were then immersed in a dilution series of polyclonal sera, with known FMDV-
818 specific IgG concentrations, from mice taken at 7, 14 or 21 dpi with FMDV for 1200 s in the
819 association phase. Subsequently, the sensors were immersed in HBS-EP buffer for 1200 s in
820 the dissociation phase. Unloaded sensors and reference wells were used to subtract non-
821 specific binding. Mean K_D (M) values were obtained from the dilution series of each mouse
822 based on their global fit to a bivalent model, with a full R^2 value of ≥ 0.9 . The K_D values were
823 measured using the ratio of k_{off}/k_{on} , to determine the avidity of antibodies in the polyclonal
824 serum samples to the FMD VLP. The values were expressed as $-\text{Log}_{10}$ of K_D (M) values,
825 and sera which had a response rate below 0 were recorded as 0.

826 **Statistical analysis**

827 The comparisons between the experimental groups and their corresponding control
828 groups were carried out using Minitab software (Minitab, US). The non-parametric Mann-
829 Whitney U test was used to compare the medians of viremia, presence of antigen, antibody
830 titres and avidities and splenic cell subsets between the 4B2 and IgG1 treated groups. A P
831 value of ≤ 0.05 was considered statistically significant.

832 **Conflict of interest statement**

833 None of the authors of this paper has a financial or personal relationship with other
834 people or organizations that could inappropriately influence or bias the content of the paper.

835 **Acknowledgments**

836 We thank The Pirbright Institute animal services team, in particular David Selby, for
837 their help with the *in vivo* procedures; Andrew Shaw and Holly Everest (The Pirbright Institute)
838 for their guidance with the Octet; Barry Bradford (The Roslin Institute, University of
839 Edinburgh) for his help with ImageJ; the bioimaging team (The Pirbright Institute), namely
840 Jennifer Simpson and the flow cytometry facility (The Pirbright Institute). For the purpose of
841 open access, the authors have applied a Creative Commons Attribution (CC BY) licence to any
842 Author Accepted Manuscript version arising from this submission.

843 **Author Contributions**

844 Conceived and designed the experiments: LG EP NM BC. Performed and analysed the
845 data: LG EP JW. Contributed reagents/materials/analysis tools: LG EP BC LK JW. Wrote the
846 paper: LG. Revised the draft for important intellectual content: BC EP NJ NM JW LK.
847 Approved the final version for publication: LG BC EP NM NJ JW LK.

References

- 849 1. Alexandersen S, Zhang Z, Donaldson AI. Aspects of the persistence of foot-and-mouth
850 disease virus in animals--the carrier problem. *Microbes Infect.* 2002;4(10):1099-110.
- 851 2. Arzt J, Belsham GJ, Lohse L, Botner A, Stenfeldt C. Transmission of Foot-and-Mouth Disease
852 from Persistently Infected Carrier Cattle to Naive Cattle via Transfer of Oropharyngeal Fluid.
853 *mSphere.* 2018;3(5):e00365-18.
- 854 3. Suttmoller P, Gaggero A. Foot-and mouth diseases carriers. *Vet Rec.* 1965;77(33):968-9.
- 855 4. Condy JB, Hedger RS, Hamblin C, Barnett IT. The duration of the foot-and-mouth disease
856 virus carrier state in African buffalo (i) in the individual animal and (ii) in a free-living herd. *Comp*
857 *Immunol Microbiol Infect Dis.* 1985;8(3-4):259-65.
- 858 5. Hedger RS. Foot-and-mouth disease and the African buffalo (*Syncerus caffer*). *J Comp Pathol.*
859 1972;82(1):19-28.
- 860 6. Alexandersen S, Zhang Z, Donaldson AI, Garland AJ. The pathogenesis and diagnosis of foot-
861 and-mouth disease. *J Comp Pathol.* 2003;129(1):1-36.
- 862 7. Jolles A, Gorsich E, Gubbins S, Beechler B, Buss P, Juleff N, et al. Endemic persistence of a
863 highly contagious pathogen: Foot-and-mouth disease in its wildlife host. *Science.*
864 2021;374(6563):104-9.
- 865 8. Anderson EC, Doughty WJ, Anderson J, Paling R. The pathogenesis of foot-and-mouth
866 disease in the African buffalo (*Syncerus caffer*) and the role of this species in the epidemiology of the
867 disease in Kenya. *J Comp Pathol*
868 1979;89(4):541-9.
- 869 9. Stenfeldt C, Eschbaumer M, Rekant SI, Pacheco JM, Smoliga GR, Hartwig EJ, et al. The Foot-
870 and-Mouth Disease Carrier State Divergence in Cattle. *J Virol.* 2016;90(14):6344-64.
- 871 10. Cunliffe HR. Observations on the Duration of Immunity in Cattle after Experimental Infection
872 with Foot-and-Mouth Disease Virus. *Cornell Vet.* 1964;54:501-10.
- 873 11. Juleff N, Windsor M, Lefevre EA, Gubbins S, Hamblin P, Reid E, et al. Foot-and-mouth disease
874 virus can induce a specific and rapid CD4+ T-cell-independent neutralizing and isotype class-switched
875 antibody response in naive cattle. *J Virol.* 2009;83(8):3626-36.
- 876 12. Carr BV, Lefevre EA, Windsor MA, Inghese C, Gubbins S, Prentice H, et al. CD4+ T-cell
877 responses to foot-and-mouth disease virus in vaccinated cattle. *J Gen Virol.* 2013;94(Pt 1):97-107.
- 878 13. Grant CFJ, Carr BV, Singanallur NB, Morris J, Gubbins S, Hudelet P, et al. The B-cell response
879 to foot-and-mouth-disease virus in cattle following vaccination and live-virus challenge. *J Gen Virol.*
880 2016;97(9):2201-9.
- 881 14. Heesters BA, Chatterjee P, Kim YA, Gonzalez SF, Kuligowski MP, Kirchhausen T, et al.
882 Endocytosis and recycling of immune complexes by follicular dendritic cells enhances B cell antigen
883 binding and activation. *Immunity.* 2013;38(6):1164-75.
- 884 15. Carroll MC. The role of complement and complement receptors in induction and regulation
885 of immunity. *Annu Rev Immunol.* 1998;16(1):545-68.
- 886 16. Imal Y, Yamakawa M. Morphology, function and pathology of follicular dendritic cells. *Pathol*
887 *Int.* 1996;46(11):807-33.
- 888 17. Heesters BA, Myers RC, Carroll MC. Follicular dendritic cells: dynamic antigen libraries. *Nat*
889 *Rev Immunol.* 2014;14(7):495-504.
- 890 18. Aguzzi A, Kranich J, Krautler NJ. Follicular dendritic cells: origin, phenotype, and function in
891 health and disease. *Trends Immunol.* 2014;35(3):105-13.
- 892 19. Carroll MC. Complement and humoral immunity. *Vaccine.* 2008;26 Suppl 8(0 8):I28-33.
- 893 20. Bachmann MF, Odermatt B, Hengartner H, Zinkernagel RM. Induction of long-lived germinal
894 centers associated with persisting antigen after viral infection. *J Exp Med.* 1996;183(5):2259-69.

- 895 21. Fray MD, Supple EA, Morrison WI, Charleston B. Germinal centre localization of bovine viral
896 diarrhoea virus in persistently infected animals. *J Gen Virol.* 2000;81(Pt 7):1669-73.
- 897 22. McCulloch L, Brown KL, Bradford BM, Hopkins J, Bailey M, Rajewsky K, et al. Follicular
898 Dendritic Cell-Specific Prion Protein (PrP^c) Expression Alone Is Sufficient to Sustain Prion Infection in
899 the Spleen. *Plos Pathogens.* 2011;7(12).
- 900 23. Heesters BA, Lindqvist M, Vagefi PA, Scully EP, Schildberg FA, Altfeld M, et al. Follicular
901 Dendritic Cells Retain Infectious HIV in Cycling Endosomes. *PLoS Pathog.* 2015;11(12):e1005285.
- 902 24. Juleff N, Windsor M, Reid E, Seago J, Zhang Z, Monaghan P, et al. Foot-and-mouth disease
903 virus persists in the light zone of germinal centres. *Plos One.* 2008;3(10):e3434.
- 904 25. Stenfeldt C, Hartwig EJ, Smoliga GR, Palinski R, Silva EB, Bertram MR, et al. Contact Challenge
905 of Cattle with Foot-and-Mouth Disease Virus Validates the Role of the Nasopharyngeal Epithelium as
906 the Site of Primary and Persistent Infection. *mSphere.* 2018;3(6):e00493-18.
- 907 26. Maree F, de Klerk-Lorist LM, Gubbins S, Zhang F, Seago J, Perez-Martin E, et al. Differential
908 Persistence of Foot-and-Mouth Disease Virus in African Buffalo Is Related to Virus Virulence. *J Virol.*
909 2016;90(10):5132-40.
- 910 27. Mabbott NA, Bruce ME, Botto M, Walport MJ, Pepys MB. Temporary depletion of
911 complement component C3 or genetic deficiency of C1q significantly delays onset of scrapie. *Nat*
912 *Med.* 2001;7(4):485-7.
- 913 28. Klein MA, Kaeser PS, Schwarz P, Weyd H, Xenarios I, Zinkernagel RM, et al. Complement
914 facilitates early prion pathogenesis. *Nat Med.* 2001;7(4):488-92.
- 915 29. Ho J, Moir S, Kulik L, Malaspina A, Donoghue ET, Miller NJ, et al. Role for CD21 in the
916 establishment of an extracellular HIV reservoir in lymphoid tissues. *J Immunol.* 2007;178(11):6968-
917 74.
- 918 30. Habiela M, Seago J, Perez-Martin E, Waters R, Windsor M, Salguero FJ, et al. Laboratory
919 animal models to study foot-and-mouth disease: a review with emphasis on natural and vaccine-
920 induced immunity. *J Gen Virol.* 2014;95(Pt 11):2329-45.
- 921 31. Doudo MHA. THE ROLE OF FOLLICULAR DENDRITIC CELLS AND PERSISTING FOOT-AND-
922 MOUTH DISEASE VIRUS ANTIGENS AS DETERMINANTS OF IMMUNE RESPONSES TO THE VIRUS:
923 University of Cambridge; 2017.
- 924 32. Kulik L, Hewitt FB, Willis VC, Rodriguez R, Tomlinson S, Holers VM. A new mouse anti-mouse
925 complement receptor type 2 and 1 (CR2/CR1) monoclonal antibody as a tool to study receptor
926 involvement in chronic models of immune responses and disease. *Mol Immunol.* 2015;63(2):479-88.
- 927 33. McCulloch L, Brown KL, Bradford BM, Hopkins J, Bailey M, Rajewsky K, et al. Follicular
928 dendritic cell-specific prion protein (PrP) expression alone is sufficient to sustain prion infection in
929 the spleen. *PLoS Pathog.* 2011;7(12):e1002402.
- 930 34. Inman CF, Rees LE, Barker E, Haverson K, Stokes CR, Bailey M. Validation of computer-
931 assisted, pixel-based analysis of multiple-colour immunofluorescence histology. *J Immunol Methods.*
932 2005;302(1-2):156-67.
- 933 35. Victoratos P, Lagnel J, Tzima S, Alimzhanov MB, Rajewsky K, Pasparakis M, et al. FDC-specific
934 functions of p55TNFR and IKK2 in the development of FDC networks and of antibody responses.
935 *Immunity.* 2006;24(1):65-77.
- 936 36. Zamorano P, Wigdorovitz A, Perez-Filgueira M, Carrillo C, Escribano JM, Sadir AM, et al. A 10-
937 amino-acid linear sequence of VP1 of foot and mouth disease virus containing B- and T-cell epitopes
938 induces protection in mice. *Virology.* 1995;212(2):614-21.
- 939 37. Rodriguez LL, Barrera J, Kramer E, Lubroth J, Brown F, Golde WT. A synthetic peptide
940 containing the consensus sequence of the G-H loop region of foot-and-mouth disease virus type-O
941 VP1 and a promiscuous T-helper epitope induces peptide-specific antibodies but fails to protect
942 cattle against viral challenge. *Vaccine.* 2003;21(25-26):3751-6.
- 943 38. Qin D, Wu J, Vora KA, Ravetch JV, Szakal AK, Manser T, et al. Fc gamma receptor IIB on
944 follicular dendritic cells regulates the B cell recall response. *J Immunol.* 2000;164(12):6268-75.

945 39. Ochsenbein AF, Pinschewer DD, Odermatt B, Carroll MC, Hengartner H, Zinkernagel RM.
946 Protective T cell-independent antiviral antibody responses are dependent on complement. *J Exp*
947 *Med.* 1999;190(8):1165-74.

948 40. Jacobson AC, Weis JH. Comparative functional evolution of human and mouse CR1 and CR2.
949 *J Immunol.* 2008;181(5):2953-9.

950 41. Chen Z, Korolov SB, Gendelman M, Carroll MC, Kelsoe G. Humoral immune responses in Cr2-
951 *-/-* mice: enhanced affinity maturation but impaired antibody persistence. *J Immunol.*
952 2000;164(9):4522-32.

953 42. Molina H, Holers VM, Li B, Fung Y, Mariathasan S, Goellner J, et al. Markedly impaired
954 humoral immune response in mice deficient in complement receptors 1 and 2. *Proc Natl Acad Sci U S*
955 *A.* 1996;93(8):3357-61.

956 43. Anania JC, Westin A, Adler J, Heyman B. A Novel Image Analysis Approach Reveals a Role for
957 Complement Receptors 1 and 2 in Follicular Dendritic Cell Organization in Germinal Centers. *Front*
958 *Immunol.* 2021;12(1136):655753.

959 44. Pikor NB, Morbe U, Lutge M, Gil-Cruz C, Perez-Shibayama C, Novkovic M, et al. Remodeling
960 of light and dark zone follicular dendritic cells governs germinal center responses. *Nat Immunol.*
961 2020;21(6):649-59.

962 45. Ahearn JM, Fischer MB, Croix D, Goerg S, Ma M, Xia J, et al. Disruption of the Cr2 locus
963 results in a reduction in B-1a cells and in an impaired B cell response to T-dependent antigen.
964 *Immunity.* 1996;4(3):251-62.

965 46. Barrington RA, Pozdnyakova O, Zafari MR, Benjamin CD, Carroll MC. B lymphocyte memory:
966 role of stromal cell complement and FcγRIIB receptors. *J Exp Med.* 2002;196(9):1189-99.

967 47. Fang YF, Xu CG, Fu YX, Holers VM, Molina H. Expression of complement receptors 1 and 2 on
968 follicular dendritic cells is necessary for the generation of a strong antigen-specific IgG response. *J*
969 *Immunol*
970 1998;160(11):5273-9.

971 48. Nielsen CH, Fischer EM, Leslie RG. The role of complement in the acquired immune
972 response. *Immunology.* 2000;100(1):4-12.

973 49. Dempsey PW, Allison ME, Akkaraju S, Goodnow CC, Fearon DT. C3d of complement as a
974 molecular adjuvant: bridging innate and acquired immunity. *Science.* 1996;271(5247):348-50.

975 50. Ross TM, Xu Y, Bright RA, Robinson HL. C3d enhancement of antibodies to hemagglutinin
976 accelerates protection against influenza virus challenge. *Nat Immunol.* 2000;1(2):127-31.

977 51. Smith KGC, Hewitson TD, Nossal GJV, Tarlinton DM. The phenotype and fate of the antibody-
978 forming cells of the splenic foci. *Eur J Immunol*
979 1996;26(2):444-8.

980 52. Dal Porto JM, Haberman AM, Shlomchik MJ, Kelsoe G. Antigen Drives Very Low Affinity B
981 Cells to Become Plasmacytes and Enter Germinal Centers. *J Immunol*
982 1998;161(10):5373-81.

983 53. Phan TG, Paus D, Chan TD, Turner ML, Nutt SL, Basten A, et al. High affinity germinal
984 center B cells are actively selected into the plasma cell compartment. *J Exp Med*
985 2006;203(11):2419-24.

986 54. Fink K, Manjarrez-Orduño N, Schildknecht A, Weber J, Senn BM, Zinkernagel RM, et al. B Cell
987 Activation State-Governed Formation of Germinal Centers following Viral Infection. *J Immunol*
988 2007;179(9):5877-85.

989 55. Smith KG, Light A, Nossal GJ, Tarlinton DM. The extent of affinity maturation differs between
990 the memory and antibody-forming cell compartments in the primary immune response. *EMBO J.*
991 1997;16(11):2996-3006.

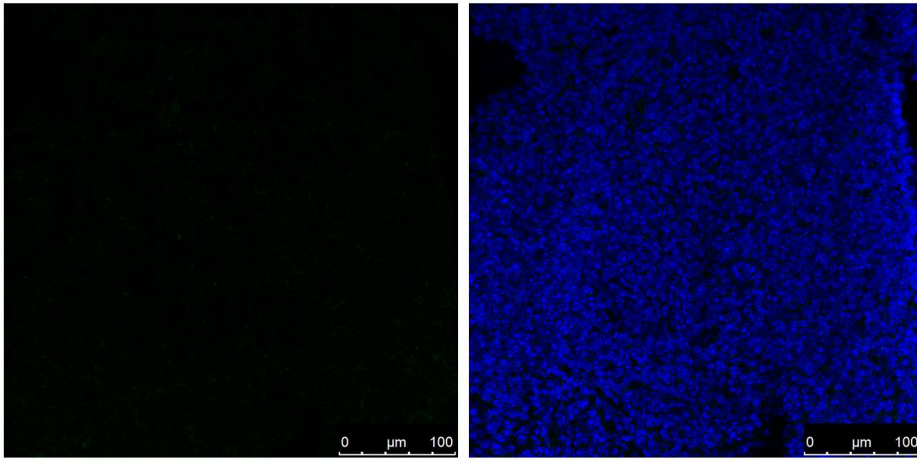
992 56. MacLennan ICM, Toellner K-M, Cunningham AF, Serre K, Sze DM-Y, Zúñiga E, et al.
993 Extrafollicular antibody responses. *Immunol Rev*
994 2003;194(1):8-18.
995 57. Shlomchik MJ, Luo W, Weisel F. Linking signaling and selection in the germinal center.
996 *Immunol Rev*. 2019;288(1):49-63.
997 58. Elsner RA, Shlomchik MJ. Germinal Center and Extrafollicular B Cell Responses in
998 Vaccination, Immunity, and Autoimmunity. *Immunity*. 2020;53(6):1136-50.
999 59. King DP, Ferris NP, Shaw AE, Reid SM, Hutchings GH, Giuffre AC, et al. Detection of foot-and-
1000 mouth disease virus: comparative diagnostic sensitivity of two independent real-time reverse
1001 transcription-polymerase chain reaction assays. *J Vet Diagn Invest*. 2006;18(1):93-7.
1002 60. Proudnikov D, Yuferov V, Zhou Y, LaForge KS, Ho A, Kreek MJ. Optimizing primer--probe
1003 design for fluorescent PCR. *J Neurosci Methods*. 2003;123(1):31-45.
1004 61. Afonina IA, Mills A, Sanders S, Kulchenko A, Dempcy R, Lokhov S, et al. Improved bplex
1005 quantitative real-time polymerase chain reaction with modified primers for gene expression analysis.
1006 *Oligonucleotides*. 2006;16(4):395-403.
1007 62. Harmsen MM, Fijten HP, Westra DF, Coco-Martin JM. Effect of thiomersal on dissociation of
1008 intact (146S) foot-and-mouth disease virions into 12S particles as assessed by novel ELISAs specific
1009 for either 146S or 12S particles. *Vaccine*. 2011;29(15):2682-90.
1010 63. Kärber G. Beitrag zur kollektiven Behandlung pharmakologischer Reihenversuche. *Naunyn-
1011 Schmiedebergs Archiv für Experimentelle Pathologie und Pharmakologie*. 1931;162(4):480-3.
1012 64. Aggarwal N, Zhang Z, Cox S, Statham R, Alexandersen S, Kitching RP, et al. Experimental
1013 studies with foot-and-mouth disease virus, strain O, responsible for the 2001 epidemic in the United
1014 Kingdom. *Vaccine*. 2002;20(19-20):2508-15.
1015 65. Cox SJ, Voyce C, Parida S, Reid SM, Hamblin PA, Paton DJ, et al. Protection against direct-
1016 contact challenge following emergency FMD vaccination of cattle and the effect on virus excretion
1017 from the oropharynx. *Vaccine*. 2005;23(9):1106-13.
1018 66. Knowles NJ, Samuel AR, Davies PR, Midgley RJ, Valarcher JF. Pandemic strain of foot-and-
1019 mouth disease virus serotype O. *Emerg Infect Dis*. 2005;11(12):1887-93.
1020 67. Dennison SM, Reichartz M, Seaton KE, Dutta S, Wille-Reece U, Hill AVS, et al. Qualified
1021 Biolayer Interferometry Avidity Measurements Distinguish the Heterogeneity of Antibody
1022 Interactions with Plasmodium falciparum Circumsporozoite Protein Antigens. *J Immunol*.
1023 2018;201(4):1315-26.
1024 68. Tsuji I, Dominguez D, Egan MA, Dean HJ. Development of a novel assay to assess the avidity
1025 of dengue virus-specific antibodies elicited in response to a tetravalent dengue vaccine. *J Infect Dis*.
1026 2021.
1027 69. Porta C, Kotecha A, Burman A, Jackson T, Ren J, Loureiro S, et al. Rational engineering of
1028 recombinant picornavirus capsids to produce safe, protective vaccine antigen. *PLoS Pathog*.
1029 2013;9(3):e1003255.

1030 Supplementary information

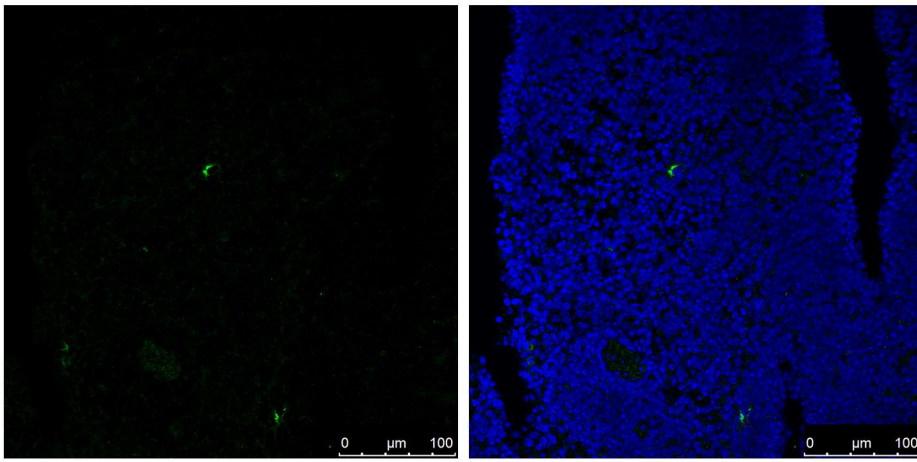
1031 Table S.1: A summary list of the animals used in the *in vivo* CR2/CR1-blockade experiment
1032 and their corresponding results

1033

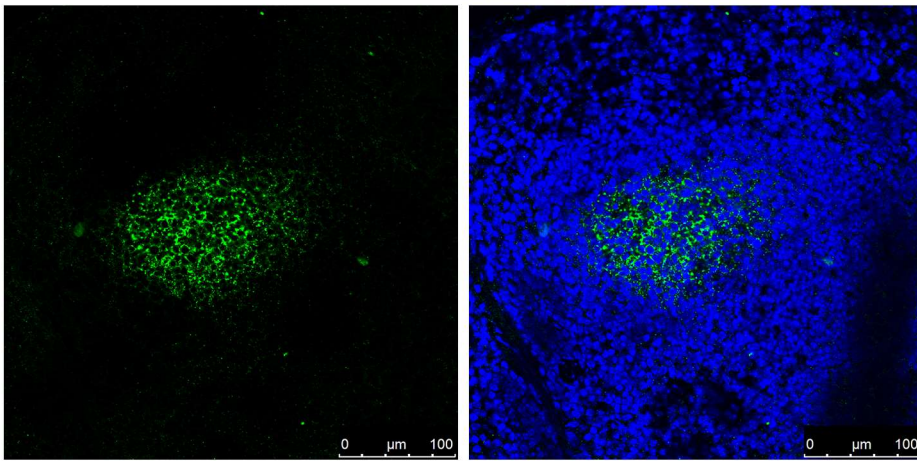
A



B



C

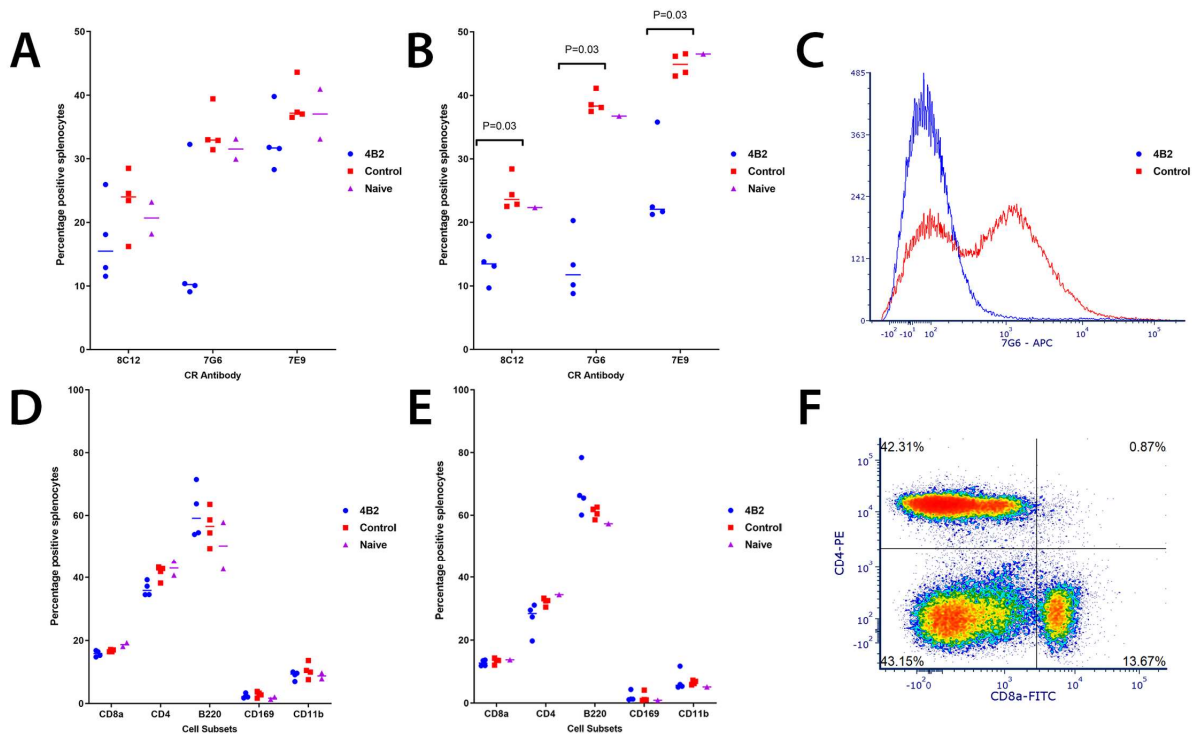


1034

1035

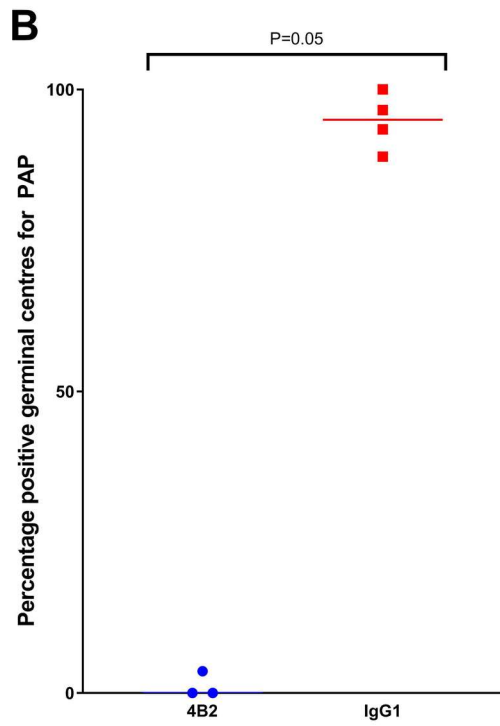
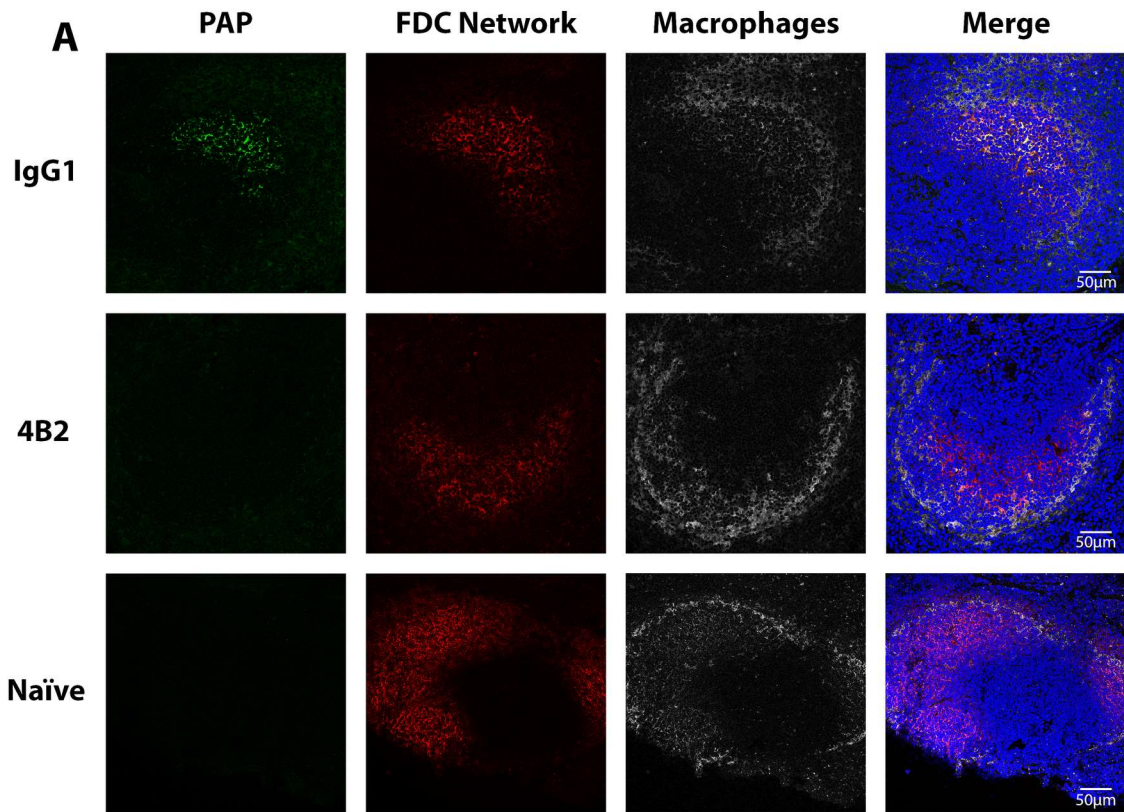
1036

1037



1038

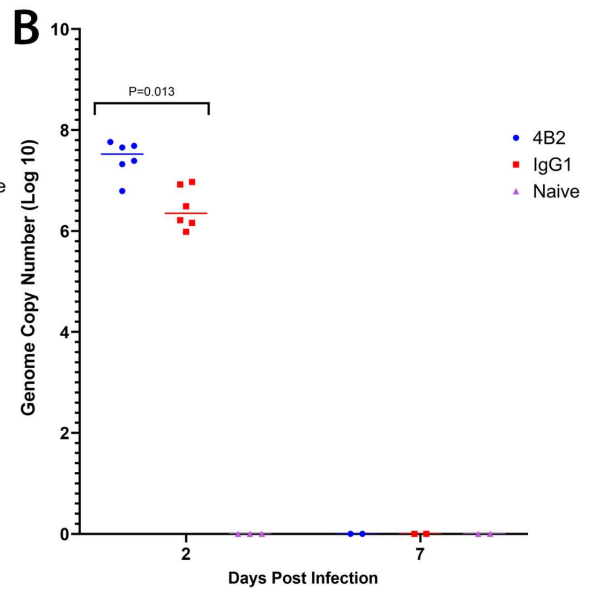
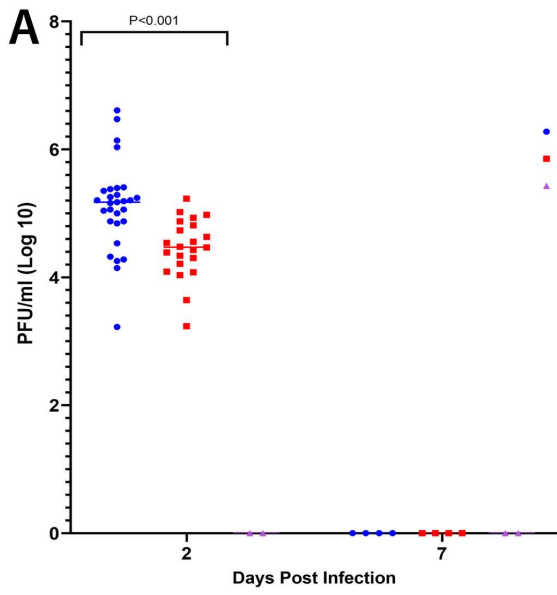
1039



1040

1041

1042

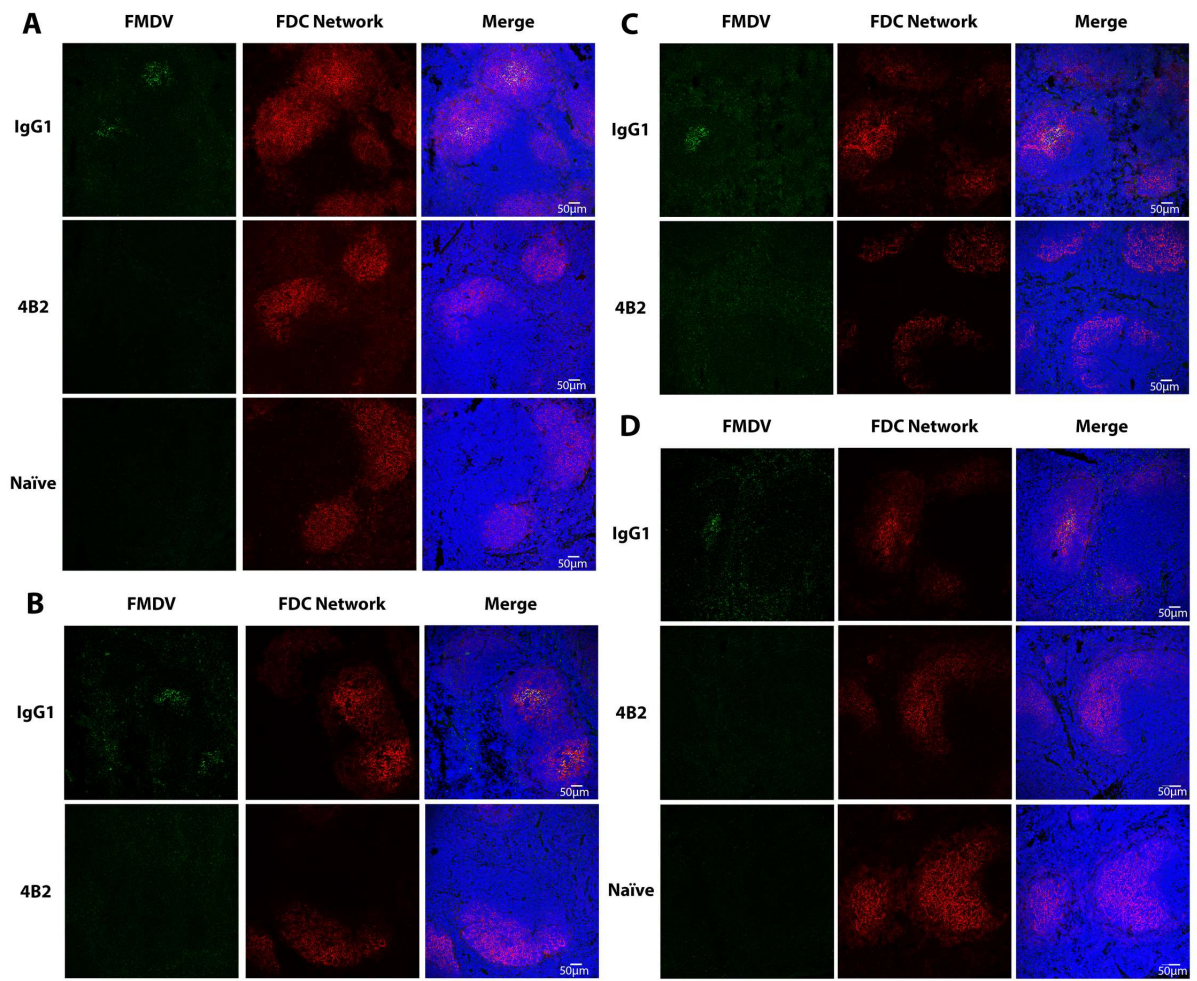


1043

1044

1045

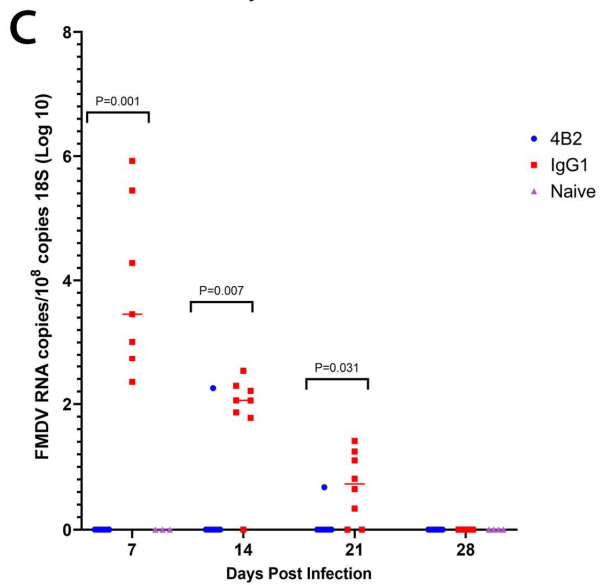
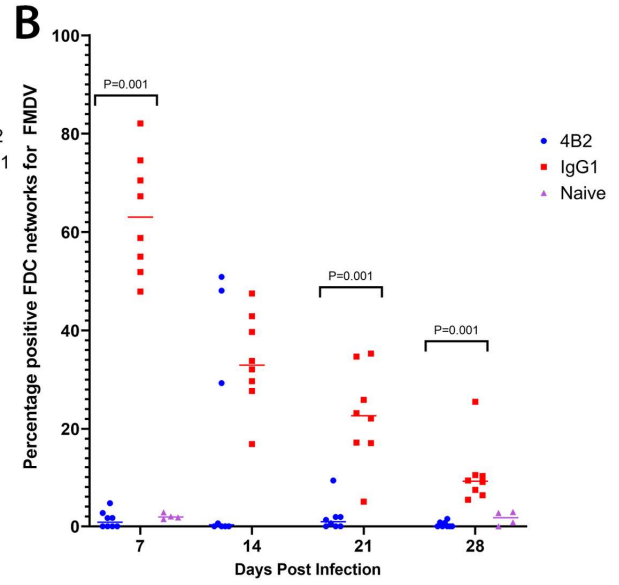
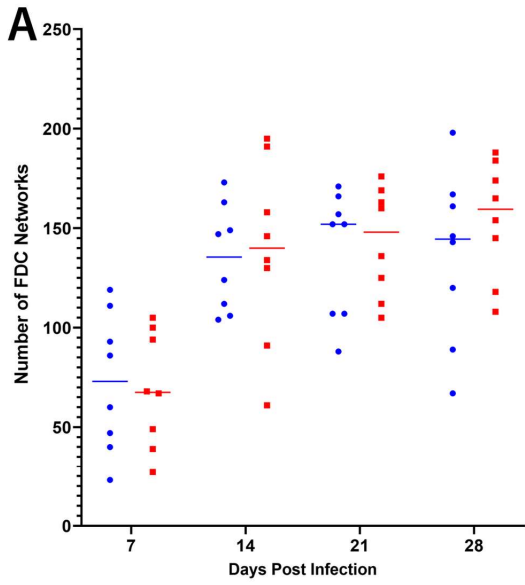
1046



1047

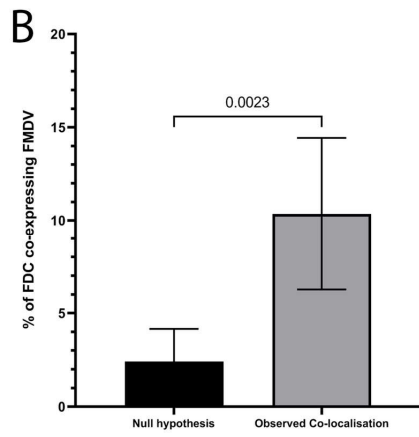
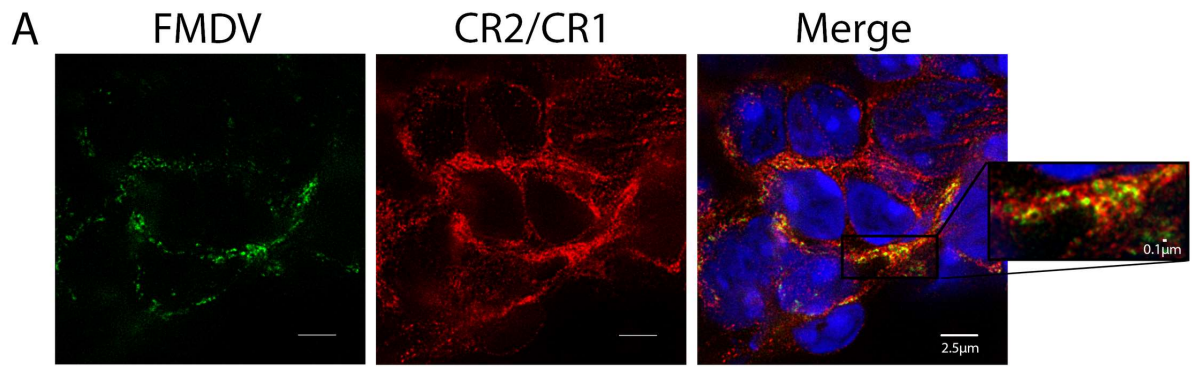
1048

1049



1050

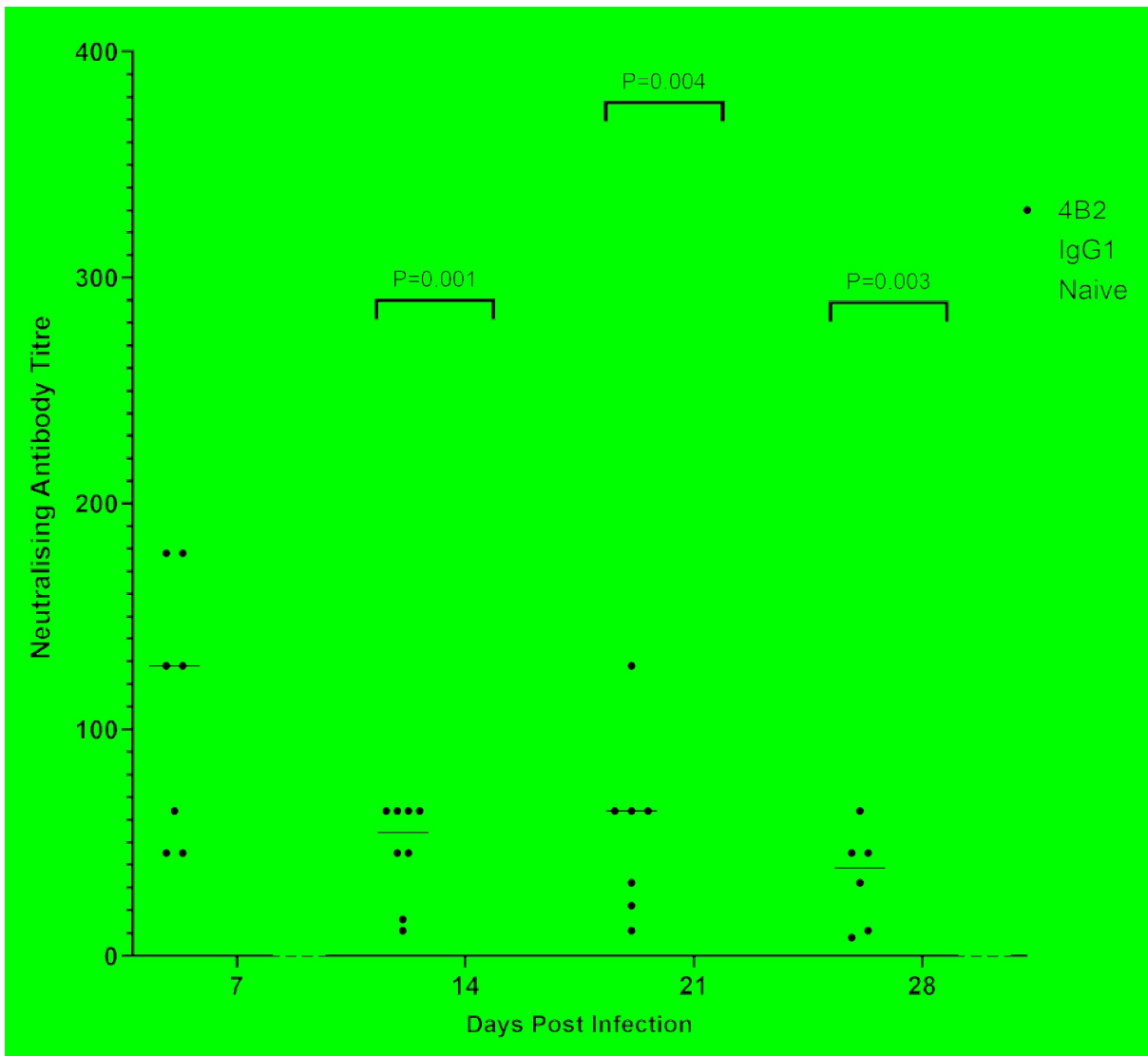
1051



1052

1053

1054

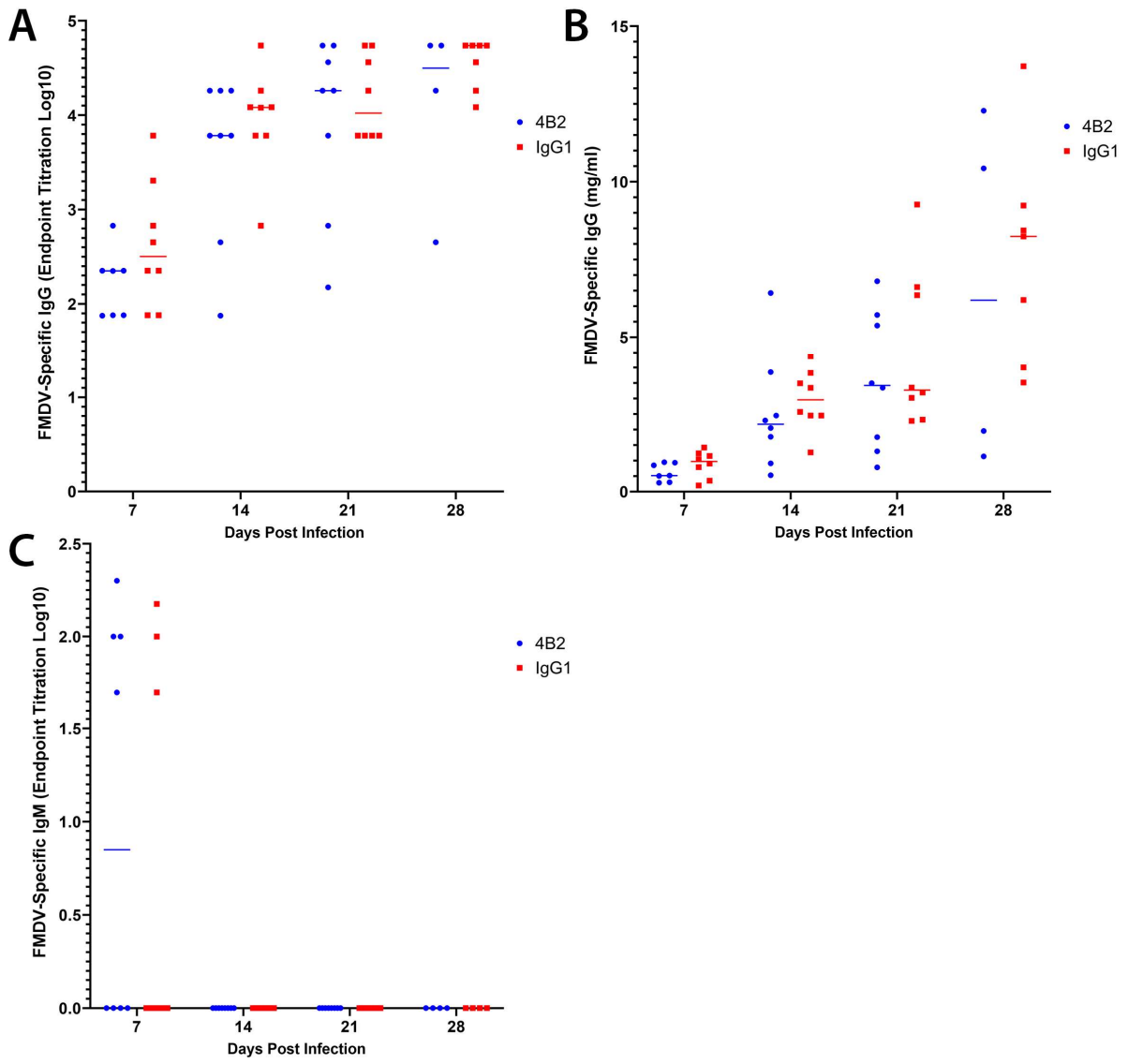


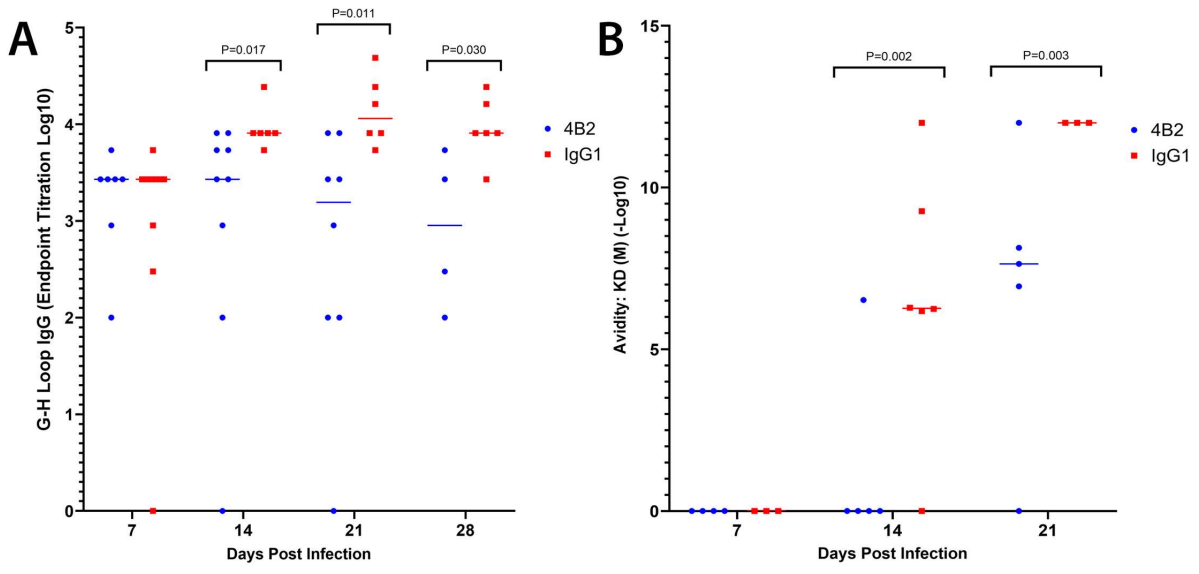
1055

1056

1057

1058





1062

1063